QUANTUM ASTROPHYSICS GENERAL FORMALISMS THEORETICAL TO EXPERIMENTAL GAGING

Abstract

The author has summarized the PHYSICS gist of advances made in the last decade having back to the blackboard examination of the inconsistencies within major branches, especially quantum and relativistic mechanics quantifying quantum astrophysical nature with physical process mechanism operating universe or universes concomitantly. Most of the PHYSICS formalisms theoretical mathematical modeling results the author has peer-published highlights have been emphasized providing wide variety of graphics to conceptualize as well as establish explanations on a broader basis. Specifically, original Helmholtz point decomposition fields modeling Iyer Markoulakis matrix formalisms that have been thereby successfully gaged having "Stringmetrics" formulation to explain fermionic fields gradient working conjunction with particle vortex fields to proceed problem solving mechanics. The author has advanced further to identify mechanisms that operate at the Planck quantum level such as Hod-PDP rotational circuit "perpetual motion machine" like assembly to generate particles from Superluminal turbulent "Superfluids" quagmire universal noisy Plenum having perhaps monopole activated energies. Space-time surfaces compressed quantum with dipole magnetism forming to show electric tensors keeping the space fields quanta that are measurable with Poynting vectors have been graphically demonstrated. Algorithm Graphics PHYSICS matrix operationally quantifiable formulae have been thoroughly derived basically out from first

Author

Rajan Iyer
Environmental Materials Theoretical Physicist
Department of Physical Mathematics Sciences
Engineering Project Technologies Engineering in International Operational Teknet Earth Global
Arizona, United States of America.

principles quantifying Hamiltonian Hermitian Higgs Coulomb gaging to arrive wavefunction, eigen spinors, signal/noise point-to-point metrics correlating with PHYSICS literature observational measurements results. Numerical achievements with operational mechanisms that are applicable for ongoing analytical modeling experimental parameters practically tabulations well discussed to take PHYSICS directionally to proper perspectives with unifying concepts having gage unitarization normalization procedures have been expounded to greater detail. The author has ansatz model introduced switches-states metrics to classify, observe, measure, analyze, and extend Standard Model metrics of charge, spin, parity, color, flavor, mass gage, and the coupling parameters to particle PHYSICS dynamic characterizations.

Progressively, the author has devised techniques with methodology to demonstrate analogous transform theoretical to macroscopic simple examples of applied problem-solving physics normal observables experimentation measurement schema. Quantum Gravity Modified Newtonian Dynamics PHYSICS Discontinuum Modeling of Nonlinear Time Rotational Space Gauge Fields Algorithm Numeration Matrix that are computer simulation programmable metrics have been originally developed by general transforms having Lagrange, Hamiltonian, Laplace, Legendre, Fourier, and Jacobian mathematical transforms have been incorporated to generalize universal observer physics black-box nature.

Prototype set-ups, figures, variable measuring instrumentation systems feasible Experimental Designs sketch graphical blueprint engineering technological advances that the author has achieved have been layout explained.

PHYSICS results from computer programming of matrix value numerical Algorithm IT coding with short discussions that the author has accumulated over these years are highlighted. Strong gravity versus weak gravity thesis PHYSICS quantifying gravitational physics dense fibers transforms propositions with synthesis of strong and the weak interactive particle spectra of vacuum baryons, quark-gluon-plasma, with gravitonic mesons evolution processes as well as Planck Quantum Point PHYSICS Vortex Gradient Fields Structures have been extended to explain how unifying field particle theories may be achieved eventually.

Keywords: Prototype set-ups, figures, variable measuring instrumentation systems feasible.

I. INTRODUCTION

We will start briefly elucidating the history of PHYSICS, specifically the role of PHYSICS, particularly theoretical practically deriving experimentally provable verifiable observables. Since that is extensive thesis having large number of references, listing literature surveys are given at the end [1-92] and no referential aspects like a paper article will be attempted here to make it like review editorial that will help reader to understand material without having to constantly refer every paragraph. Here, the chapter thesis represents a very short compilation of key PHYSICS progressively advanced by scientists, especially physicists who are Nobel Laureates. History of physics summarized here spans over three centuries of careful theoretical and experimental scientific physics works with in-depth thought, philosophy, logic, practical sense, painstakingly keen observations objectively, clever instrumentation measurements with precision and extreme accuracies, as well as hypothetical testing, proof, verifications, with mathematical abstractness, as well as physical clarity.

Progressive understanding of PHYSICS starting with Galileo, then Newton and other scientists eventually extended one-dimensional descriptions to more than one dimensional to conform to proper geometry of universe. Three-dimensional Euclidean geometric PHYSICS helped to understand natural processes; however, space-time required four-dimensional topology and then manifolds of higher dimensions necessitated with String and Super String theories. Still, there had been many questions and paradoxes unanswered, although basic geometric physics was extended to higher dimensional matrix tensor forms. Classical PHYSICS manifesting energy and matter successfully quantifiably formulated conservation gist four laws of thermodynamics stating a set of principles that describe how energy and entropy behave in thermodynamic systems. Statistical mechanics quantified entropy, measuring the degree of the disorder or randomness in a system, within the form S = k * ln W, where S is the entropy, k is the Boltzmann constant, ln is the natural logarithm, and W is the number of microstates. This equation additionally showed that entropy to be a measure of uncertainty or information content of a system helped to define arrow of time. The higher the entropy, the less information we might gather about the exact state of the system and could be used as also measure of information loss or noise in a communication process.

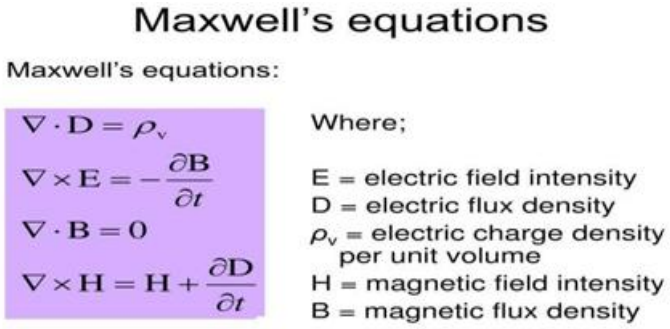

Maxwell provided electromagnetic light mathematical field theory with these equations that describe how electric and magnetic fields might get generated and interact with each other as well as with electric charges and currents. One of the key results that became cornerstone of Einstein's Special Theory of Relativity and equivalence principle was

constancy of the speed of light: $c = 1/\sqrt{\mu 0 \varepsilon o}$, which is equal to the speed of light measured by experiments, with $\mu 0$: permeability of free space and εo: permittivity of free space. Maxwell's theory laid the foundation for modern physics and technology, such as radio, television, radar, lasers, fiber optics, wireless communication, and transmitting-receiving information waves.

Quantum Mechanics was developed by many 20th century physicists, like Planck, Bohr, Einstein indirectly, Schrödinger, Pauli, Dirac, and Heisenberg. Quantum physics had brought out that physical quantities, such as energy, momentum, angular momentum, electric charge, and particle spin can only take discrete values, called quanta. Quantum physics also further introduced concepts of wave-particle duality, uncertainty principle, superposition principle, entanglement, and many others that challenge the commonsense notions of reality, historically traced back to Kirchhoff's discovery of black body radiation. Planck quantized light in the units of hf, where h is Planck's constant, and f is radiation frequency, explaining observed distribution of radiation emitted by a hot object, which could not be accounted for by classical physics.

In 1905, Einstein extended Planck's idea to explain the photoelectric effect, which Einstein quantified to be emission of electrons from a metal surface when exposed to light photons. In 1913, Bohr developed a model of the hydrogen atom that incorporated both classical and quantum physics. He postulated that electrons could be jumping from one orbit to another by absorbing or emitting photons with energy equal to the difference between the orbital energies, especially with hydrogen atom energy levels correlating experimental observations. Schrödinger and Heisenberg in 1925-1926 independently formulated two equivalent versions of quantum mechanics: wave mechanics and matrix mechanics. Heisenberg introduced a matrix representation of physical observables and their commutation relations of uncertainty principle which stated about a fundamental limit to how precisely one might measure two incompatible observables, such as position and momentum via equation: $\Delta x.\Delta p \geq h/4\pi$, where Δx = positional change, Δp = momentum change measurements having uncertainty at least $h/4\pi$, with h = Planck's constant. It further also implied that there would be a fundamental limit to how much information, in terms of quantum probabilities one might extract from a quantum system, and that some information might get irretrievably lost in the process of measurement. Pauli proposed an exclusion principle stating that no two identical fermions (particles with half-integer spin) can occupy the same quantum state in a system. Dirac thereby combined quantum mechanics with special relativity to obtain a relativistic wave equation of the electrons, predicting antimatter existence possibility and explained electron spin processes.

Einstein's Special Theory of Relativity showed that space and time wouldn't be absolute, but relative to the state of motion of the observer. It also quantified mass-energy equivalence, according to the famous equation E = mc^2, where E = energy, m = mass, and c = speed of the light. General relativity tried to quantify theory of gravity that Einstein postulated after the Special Relativity Theory between 1907 and 1915, based on the principle that gravity was a consequence of the curvature of space and time caused by the presence of mass and energy.

General relativity showed equivalence principle that effects of gravity to be having

same as effects of acceleration, and that light could be bent, redshifted, or blue shifted on passing near massive objects. It also predicted new phenomena, such as gravitational waves, gravitational lensing, black holes, and gravitational time dilation. GRT explained many phenomena that could not be accounted for by classical physics, such as the precession of Mercury's orbit, the deflection of starlight by the Sun, the expansion of the universe, and the existence of cosmic microwave background radiation. One of the consequences of Einstein's General Theory of Relativity was predicting presence of black holes as extreme regions of gravity, having the event horizon boundary, marking the point of no return for anything that might cross it; they emit x- rays and gamma rays, that might be observed by telescopes. Black holes might often distort the light from distant stars and galaxies, creating a phenomenon known to be gravitational lensing. The first image of a supermassive black hole was taken in 2019 by the Event Horizon Telescope, showing black hole at Messier 87, a giant elliptical galaxy about 55 million light-years away.

Black holes might in general emit gravitational waves, due to ripples in space-time caused by accelerating masses, produced when two black holes merge, or when a black hole collided essentially with another compact object, such as a neutron star.

Hawking radiation would be theoretical phenomenon of black holes emitting thermal radiation, reducing their mass and energy over time, identified to be black body spectrum.

Hawking had shown that temperature of a black hole to be inversely proportional to its mass, so smaller black holes might be hotter and emit more radiation than larger ones, quantitatively:

$T_{\mathrm{H}} = \frac{\hbar c^3}{8\pi G M k_{\mathrm{B}}}$ where T_H = Hawking radiation temperature, $\hbar$ = reduced Planck's constant, c = speed of light, G = gravitational constant, M = mass of the black hole, and k_B = Boltzmann constant. Schwarzschild quantified the blackhole event horizon by the formula: $Rs = 2GM/c^2$ where Rs = Schwarzschild radius, G = gravitational constant, M = mass of the black hole, and c = speed of light. The spin and the charge of the black hole might affect the event horizon. Hypothetical black holes having very small masses and sizes, possibly as small as the Planck scale (about 10^{-35} meters and 10^{-8} kilograms) would be categorized as microblackholes, possibly created in the early universe or by high-energy collisions of particles, occurring in particle accelerators or cosmic rays. Zero-point vacuum per quantum field theory of vacuum state would be the lowest energy state of a quantum system. Microblackholes created by the fluctuations of the zero-point fields could be sources or sinks.

The matter particles and the force particles are the two primary parts of the Standard Model Particle PHYSICS. The fundamental constituents of matter are called matter particles, and they are divided into two categories: quarks and leptons. Six lepton types (electron, muon, tau, and their associated neutrinos) and six quark kinds (up, down, charm, strange, top, and bottom) exist. Quarks and leptons come in three generations, with increasing mass and decreasing stability. Quarks also have a property called color charge, that determines how they interact with strong nuclear force. The force particles are the carriers of the four fundamental forces: the electromagnetic force, the strong nuclear force, the weak nuclear force, and gravity. The electromagnetic force is mediated by light photons, which are massless and have no electric charge. Strong nuclear force is mediated by gluons, which are also massless and have no electric charge, but have color charge. The weak nuclear force is

mediated by W and Z bosons, which are massive and can be electrically charged or neutral. The Higgs field is a quantum field that fills all of space and gives mass to other particles through its interactions with them. The Higgs boson was predicted by the Standard Model in 1964, but it was only discovered in 2012 by the Large Hadron Collider at CERN laboratory.

Penrose has proposed Conformal cyclic cosmology that suggests that the universe undergoes infinite cycles of expansion and contraction, has no beginning or end, but rather goes through infinite cycles of creation and destruction. Penrose also interprets quantum mechanics to explain the collapse of the wave function because of gravity by superposition of quantum states cannot be maintained beyond a certain threshold of energy difference of one Planck mass, where gravity becomes unstable and causes a spontaneous reduction of the wave function. Penrose process describes a mechanism allowing an observer to extract energy from ergo sphere of a rotating black hole.

Parisi has proved spin glass has spins that point in different directions and can change their orientation over time, having magnetic atoms of iron mixed tonon-magnetic copper. The magnetic atoms are randomly distributed in the metal lattice, and they interact with each other through both ferromagnetic and antiferromagnetic bonds. They are models for studying other complex systems, such as neural networks, optimization problems, biological evolution, and social networks.

II. HIGHLIGHTS OF ANSATZ IYER MARKOULAKIS ADVANCED TO IMMOHZT HODPDP PHYSICS

Iyer Markoulakis point Helmholtz decomposed field theoretical modeling is a complex and advanced topic in physics and mathematics that involves the use of Helmholtz Hamiltonian mechanics to describe the dynamics of electromagnetic fields and particles. It is based on the idea that any vector field can be decomposed into a curl-free component and a divergence-free component, which are called the gradient field and the rotation field, respectively. The gradient field is a field that points in the direction of the maximum increase of a scalar function, such as the potential energy or the temperature. The vortex field is a field that has zero divergence and nonzero curl, meaning that it has no sources or sinks, but it has rotation or circulation. This is referred to as the Helmholtz representation or decomposition. Typically of any vector field may be expressed as the sum of a gradient field and a vortex field using the Helmholtz decomposition or Helmholtz representation in Iyer Markoulakis' approach. It also uses a 2x2 eigen tensor matrix to describe the dynamics of these fields and their interactions with point vortices and gradient fields, which can model the behavior of monopoles, electrons, positrons, and other quantum phenomena. The Iyer Markoulakis formalism is a mathematical framework that aims to unify the four fundamental forces of nature: gravity, electromagnetism, strong nuclear force, and weak nuclear force. The formalism extends the Coulomb-Hilbert gauge, which is a way of choosing the electric potential and the magnetic potential to simplify the Maxwell equations, to include the Higgs mass field, which is a scalar field that gives mass to elementary particles. The formalism also uses asymmetric string metrics, which are mathematical objects that describe how distances and angles are measured in curved spacetime, to account for the asymmetrical forces between magnetic poles. The Iyer Markoulakis formalism has potential applications for quantum supercomputing, quantum astrophysics, and grand unification theories. Monopoles, if they exist, could be used as qubits because they have two possible states: north or south, and these

states could be manipulated by applying electric or magnetic fields, or by exchanging photons with other monopoles; otherwise, they can be entangled with each other through their magnetic interactions. They can offer some advantages over other qubit implementations, such as having longer coherence times, higher scalability, and lower noise.

Iyer Markoulakis Malaver O'Neill Hodge Zhang Taylor gage discontinuity dissipative "Stringmetrics"Hod PDP Helmholtz decomposed point fields PHYSICS is a paradigm shifting theoretical framework that tries to unify the four fundamental forces of nature using Helmholtz decomposition and asymmetric string metrics. The framework also uses asymmetric string metrics, which are mathematical objects that describe how distances and angles are measured in curved spacetime, to account for the asymmetrical forces between magnetic poles. The Hod-PDP mechanism proposes that these particles can form stable or unstable combinations, such as dipolar pairs, loops, strings, or bundles, depending on their relative orientations and distances. Emergent quantum Hod-PDP mechanism is a very advanced and complex topic in physics and mathematics that requires further research and verification. Potentially it proposes applications for quantum supercomputing, quantum astrophysics, and grand unification theories.

1. **Statement of the Problem**: While quantum mechanics quantum field theory tries to link micro to macro physics, special general theory of relativity posits macro micro physics. However, discrepancies arise when evaluating parametrically quantum mechanics with relativity theory, especially with the vacuum energy solutions, leading to vacuum as well as ultraviolet catastrophes. These inconsistencies within major branches, especially quantum and relativistic mechanics quantifying quantum astrophysical nature with physical process mechanism operating universe or universes would necessitate ansatz novel approaches to problem solving PHYSICS. Space variables of the distance metrics tend to be discontinuous, hence no monotonic functionality may exist. The mass factor has always been a problem, especially with the well-defined Yang–Mills existence and mass gap situation, that is still an unsolved problem in mathematical physics pointing to higher mathematics advancement.

2. **Solution of the Problem:** The author elucidates here sections with roadmaps to address the solution of the problem. Observer physics has been advanced to emphasize the role of conscious observer perspectives playing the key role determining observations measurements wholly. Essentially putting together {timeline, worldline, state-of-the-clock, environment, consciousness} operator with input evolving to dynamic system quaternion imaginary throughput leading to Boolean binary output process nature is quite conceivable. Perhaps, this is how computer perceives as matrix theoretical physics synthesis of point universal pattern lattice emergence evolutions!! Starting off with micro "Quantum Gage Point Tensor Field Theory" on imaginary quaternion aspects, real formalisms having gage physical transformations that will involve fields of a sense-time-space five dimensional aspect, the following physics formalisms have been expertly peer published already. In this Chapter, this will be in gist discussed briefly.

Ansatz Iyer Markoulakis PHYSICS FORMALISM [59]

$$\begin{pmatrix} \hat{\varepsilon}_{r,\mu\nu} & \hat{\varepsilon}_{g}^{\mu\nu} \\ \hat{\varepsilon}_{g,\mu\nu} & \hat{\varepsilon}_{r}^{\mu\nu} \end{pmatrix} \quad \textbf{(1)}$$

III. HELMHOLTZ DECOMPOSED POINT S2 MATRIX, HAVING {GRADIENT, VORTEX} SPACE PARITY FIELDS[56]

To get eigenvalues of characteristic field matrix above, we equate |A-λI| = 0; hence

$$\begin{pmatrix} \varepsilon r, \mu\nu - \lambda & \varepsilon_{g}^{\mu\nu} \\ \varepsilon g, \mu\nu & \varepsilon_{r}^{\mu\nu} - \lambda \end{pmatrix} = 0 \text{ \& solving quadratic equation in } \lambda:$$

$$\lambda^2 - (\varepsilon_{r,\mu\nu} + \varepsilon_{r}^{\mu\nu})\lambda + (\varepsilon_{r,\mu\nu}\varepsilon_{r}^{\mu\nu} - \varepsilon_{g,\mu\nu}\,\varepsilon_{g}^{\mu\nu}) = 0 \quad \textbf{(2)}$$

eigenvalues will have characteristic eigenvalue solutions.

The author has shown signal/noise graphing using the above Iyer Markoulakis Physics fields point formalism to problem solving vortex energy function for attractive-repulsive energy fields to get graphic following plots. Figures 1 and 2 graphically demonstrate the effect of the vortex fields on the vacuum fluctuations. High energy density signal localized events manifest superluminal super-fluids reflecting at the boundary of the hydrodynamic like vortex rotational energy sustains Hamiltonian oscillators generating pulses, with damped oscillations as sinusoidal nonlinearity per Figure 1. It is possible to identify in Figure 2 regions of superluminal wave velocities of super-fluids, characteristically frictionless motion, without viscous flow.

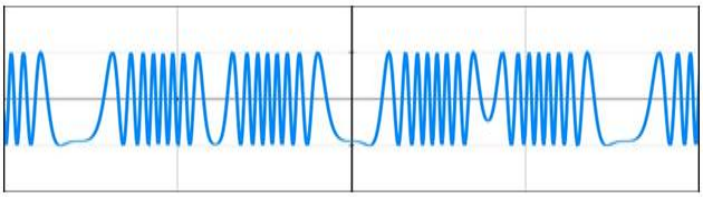

Figure 1: Graph showing vortex generators of sinusoidal pulse signals. Here, X: vortex action function; Y: sinusoidal signals, per modeling analyses using vortex form available online[59].

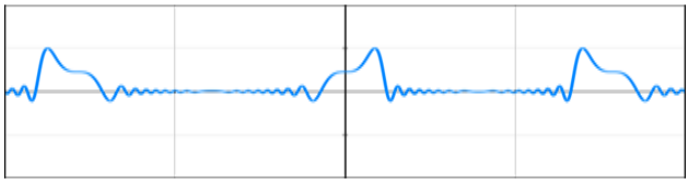

Figure 2: Graphing repulsive-attractive distance & distribution profile with equivalent wave velocity in vacuum space vortex quanta[59], using values of the electric constant=8.85418782x10- 12 m-3 kg-1 s4 A2, and magnetic constant = 1.25663706×10-6 m kg s-2 A-2, applied to the Figure 1 signals graphically per Iyer Markoulakis formalism and online available tools.

1. **Inference of Wavefunction Collapse within Micro-Wormhole**: Quantum manifolds linking to global vacuum space to astrophysical relativistic macro-space, short-cut path of microwormhole are possible due to collapsing wavefunction inferable in Figure 2.

   The author has shown per matrix property analysis mathematically that the following inner product and outer product relationships hold, per Hilbert space to equivalent wavefunction energy functional general forms[64]:

   <E|T> = <E|U|T>(|E><T|)-1|E>) T|T>U-1. Substituting**, E = Ψμ(t); T = Ψμ(t); U = V; |E><T| = ρ(t); <E|T> = ΨμδΨμ; <(E|U|T> = ΨμδΨμ . FE,** it gives result **FEt = ρ(t)(<Ψμ(t)|Ψμ(t)>)-1V.**

   Applying above pure mathematical results obtained by the author to quantify Coulomb Higgs gauge to deriving "string-metrics", with diagonal terms Higgs gravity like mass factor, and cross-diagonal terms like fermionic gauge coupling given by $\hat{G}$ would yield following matrix [57]:

$$\begin{pmatrix} \mathbf{0} & \widehat{\mathbf{G}} \\ \begin{pmatrix} \mathbf{0} & \widehat{\mathbf{G}} \\ \begin{pmatrix} \mathbf{0} & \widehat{\mathbf{G}} \\ \widehat{\mathbf{G}}^{-1} & \widehat{\mathbf{M}} \end{pmatrix}\mathbf{G}^{-1} & \widehat{\mathbf{M}} \end{pmatrix}\mathbf{G}^{-1} & \widehat{\mathbf{M}} \end{pmatrix}\mathbf{G}^{-1} & \widehat{\mathbf{M}} \end{pmatrix} \tag{3}$$

   Here, $\hat{G}$= (<Ψμ(t)|Ψ$^{\mu}$(t)>)$^{-1}$ $||\nabla \underset{g}{E^{\mu\nu}}||$ ρ(t) = f,ρ(t), where $\hat{G}$s the functional mathematics;

   <Ψμ(t)|Ψ$^{\mu}$(t)> gives the inner product of the lower **Ψμ(t)** and the upper **Ψ$^{\mu}$(t)** wave functions as a function of time. Gaging observables with scalar potential **V = ||∇E$^{\mu\nu}$||**, quantum density matrix ρ(t), and the function operator f transforming parametrically **ρ**(t) to $\hat{\mathbf{G}}$ gets quantified by the equation: f = (**Ψ**$_{\mu}$(t)|**Ψ**$^{\mu}$(t>)$^{-1}$ $||\nabla \mathbf{E}_{\mathbf{g}}^{\mu\nu}||$**,** or equivalently $\widehat{\mathbf{G}}$ = f.**ρ**(t)**.** Also shown earlier[67] was Γ =*signal/noise ratio, satsifying permutation summing over point latitude i and longitude j of Γ$_{ij}$:*

$$\sum_{\mathbf{i=1}}^{\mathbf{n}} \sum_{\mathbf{j=1}}^{\mathbf{m}} \mathbf{\Gamma_{ij}} = \mathbf{1} \tag{4}$$

   For example, that if $\boldsymbol{\Gamma_{ij}}$ **= [Γ] {Ψ11 Ψ12 Ψ13 …….Ψ21 Ψ22 Ψ23 }** when summed over nodes *of finite element model network circuitry assemblage values of i and j, like in Hod-PDP, i.e., the Hod-Plenum* Pauli Dirac Planck (PDP) circuit model one can utilize Equation (4).*

2. **Gage Time Gage Space Fields Probability Signal Matrix**: The author has derived relationship quantifying space gauge matrix fields and the wavefunction to signal/noise measurables with[67]:

$$\begin{pmatrix} \boldsymbol{\varepsilon_\tau} \\ \boldsymbol{\varepsilon_x} \\ \boldsymbol{\varepsilon_y} \\ \boldsymbol{\varepsilon_z} \end{pmatrix} \left(\boldsymbol{\psi_{\Gamma^{\dagger}_{\circlearrowleft}}} \;\; \boldsymbol{\psi_{\Gamma^{-}_{\vartheta}}} \;\; \boldsymbol{\psi_{\Gamma^{+}_{\vartheta}}} \; \boldsymbol{\psi_{\Gamma^{-}_{\circlearrowleft}}} \right) =>::<= \begin{pmatrix} \boldsymbol{\Gamma_t^-} & \boldsymbol{\Gamma_{X\circlearrowleft}} & \boldsymbol{\Gamma_Y^-} & \boldsymbol{\Gamma_{Z\circlearrowleft}} \\ \boldsymbol{\Gamma_t^{\vartheta}} & \boldsymbol{\Gamma_X^+} & \boldsymbol{\Gamma_Y^{\vartheta}} & \boldsymbol{\Gamma_Z^+} \\ \boldsymbol{\Gamma_t^+} & \boldsymbol{\Gamma_X^{\vartheta}} & \boldsymbol{\Gamma_Y^+} & \boldsymbol{\Gamma_Z^{\vartheta}} \\ \boldsymbol{\Gamma_{t\circlearrowleft}} & \boldsymbol{\Gamma_X^-} & \boldsymbol{\Gamma_{Y\circlearrowleft}} & \boldsymbol{\Gamma_Z^-} \end{pmatrix} \qquad \textbf{(5)}$$

or $[\boldsymbol{\Gamma_{XYZ}}] =>::<= [\boldsymbol{\Gamma_{X'Y'Z'}}] [\boldsymbol{\Gamma_{X''Y''Z''}}]$.., with $\{\boldsymbol{\Gamma_{X'Y'Z'}}, \boldsymbol{\Gamma_{X''Y''Z''}}\}> [\boldsymbol{\Gamma_{XYZ}}]$, due to Equation (4).

Equation (5) is key to interconverting signal/noise measurements to space fields – wavefunction eigen-spinors and then vice-versa. Ket vector $\begin{pmatrix} \varepsilon_\tau \\ \varepsilon_x \\ \varepsilon_y \\ \varepsilon_z \end{pmatrix}$ describes time space gauge fields of the 4 dimensional time space {t, X, Y, Z}; $\left(\psi_{\Gamma^{\dagger}_{\circlearrowleft}} \;\; \psi_{\Gamma^{-}_{\vartheta}} \;\; \psi_{\Gamma^{+}_{\vartheta}} \; \psi_{\Gamma^{-}_{\circlearrowleft}} \right)$ gives probability functions quantifying distributions of signal/noise sense {$\psi_{\Gamma^{\dagger}_{\circlearrowleft}}$ clockwise positive, $\psi_{\Gamma^{-}_{\vartheta}}$ anticlockwise negative, $\psi_{\Gamma^{+}_{\vartheta}}$ anticlockwise positive, as well as $\psi_{\Gamma^{-}_{\circlearrowleft}}$ clockwise negative}. $\begin{pmatrix} \Gamma_t^- & \Gamma_{X\circlearrowleft} & \Gamma_Y^- & \Gamma_{Z\circlearrowleft} \\ \Gamma_t^{\vartheta} & \Gamma_X^+ & \Gamma_Y^{\vartheta} & \Gamma_Z^+ \\ \Gamma_t^+ & \Gamma_X^{\vartheta} & \Gamma_Y^+ & \Gamma_Z^{\vartheta} \\ \Gamma_{t\circlearrowleft} & \Gamma_X^- & \Gamma_{Y\circlearrowleft} & \Gamma_Z^- \end{pmatrix}$ has the power to expand to a 4D time-space point matrix signal/noise distributed over Γ with {t, X, Y, Z} {- negative, + positive, ϑ anticlockwise, $\circlearrowleft$ clockwise}. If forming magic squares, each 2x2 pan-diagonal submatrices has PDP circuit cell assemblies like the molecular crystallographic observable unit cells, that may be characteristics of time crystals.

3. **Inferring Critical (Γ, ρ) Matrix Characterizing Electromagnetic Gravity:** Consider condition that, if $[\Gamma] > [\Gamma_{cr}]$, multiple phases matrices mix, or combine; if $[\Gamma] < [\Gamma_{cr}]$, then phases separate onto multiple phases matrices. Mesoscopic examples may be used to demonstrate that. For instance, these separate onto numerous liquid-solid phases, plasma to gases, mixed gases to elemental gases of hydrogen, multiphase liquids to elemental liquids and/or solid phases at low Γ values, which are typical of nebular plasmatic gases. High Γ phases joining or mixing to create more complicated forms will be another example.

IV. SCHEMATIC OF MATRIX PAULI DIRAC PLANCK CIRCUIT [60] SCHEMATIC OF FIGURE 1.

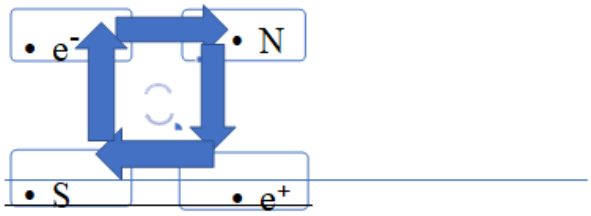

Figure 3: PDP model of Pauli Dirac Planck circuit assembly having e^-: electron and e^+: positron particles; N: north and S: south monopoles. Arrows show matrix gradient vortex flow.

Equation for this PDP circuit having $\hat{\varepsilon}_n = \hat{\varepsilon}$ and $\hat{\varepsilon}_s = \hat{\varepsilon}^*$, can be given as the eigenvector [60] matrix:

$$[\lambda_{PauliDiracPlanckcircuitgaging}] = [\lambda_{PDPcg}] = \begin{pmatrix} 1 & \mathfrak{C} \\ \mathfrak{C}* & 1 \end{pmatrix} \quad \textbf{(6)}$$

with $[\lambda_{PauliDiracPlanckcircuitgaging}]$: combinatorial eigenvector bundle matrix, $\mathfrak{C}$: scalar value of south and north monopole field, and $\mathfrak{C}*$: conjugate value of $\mathfrak{C}$ fields. Equation (6) is characterizing like Super Symmetry (SUSY), with Hermitian quantum matrix. We envision annihilation of the electron-positron pairs as well as dipolar collapses of north and south monopoles "stable" magnetism, representing quantitatively in "Stringmetrics" gage Equation (3), characterizing electromagnetic fields here. Per John Hodge's results showing forces of south poles to be slightly stronger than that of the north poles, we expect $\hat{\varepsilon}_s > \hat{\varepsilon}_n$ slightly. Considering that, $[\lambda_{PDPcg}]$ will be asymmetric strings gage metrics, a non-Hermitian quantum matrix, pointing to anisotropic eccentric precession of electromagnetic gaging fields, like electromagnetic gravity.

V. GRAPHICAL SCENARIOS ANALYSIS WITH PDP CIRCUIT ASSEMBLY [60] SPACE-TIME SURFACES PER FIGURE 10 OF THE FIGURE 5 SCENARIO

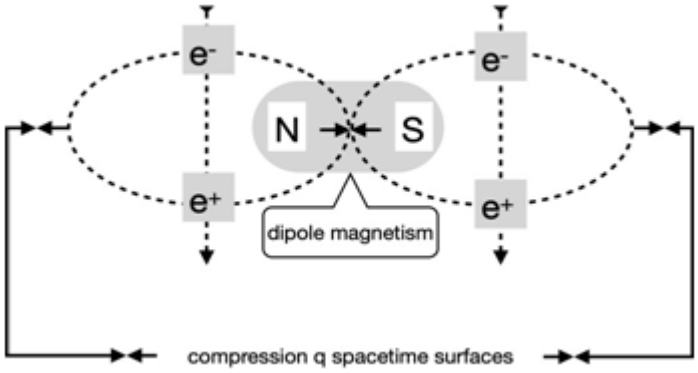

Figure 4: Schematic showing how PDP configuration may account for dipole magnetism generated due to dynamic electric tensors created out of monopole magnetic gaging fields. Space-time surfaces result from compressed quanta action interactions.

The author has explained earlier in many publications that Figure 4 above will provide the best scenario for a finite element modeling analysis with computer programming validating theory of PDP mechanism simulations. Poynting vector maybe utilized to measure electric and magnetic effect fields at each point. The Poynting vector is a quantity that describes how much energy is carried by an electromagnetic wave, such as light or radio waves. The Poynting vector is calculated by taking the cross product of the electric field and the magnetic field of the wave, divided by the permeability of the medium that the wave travels through. The direction of the Poynting vector is the same as the direction of the wave propagation, and its magnitude is proportional to the intensity of the wave. The unit of the Poynting vector is watt per square meter, which means power per unit area, formula S = (E x B) / μ0 can be used to calculate Poynting vector at any point in space appropriate to measure point-to-point signal/noise matrix.

Numerical resuls theoretical with Hod-PDP mechanism having Table of earlier graphs

Table 1: Summary with theoretical numerical results of Hod-PDP mechanism; shown are monopole mass, zero-point micro-blackhole entity sizes, estimated space-time extent, monopole core size, monopole charge, size of a fermion typically, and estimated size of Pauli-Dirac-Planck circuit monopole particle assembly. The estimated size of Pauli Dirac Planck circuitry assembly is greater than 10^{-34} Planck magnitude and less than quasi-particle size 10^{-26} metrics unit. Note value ranges are given as per the referential literature [60] Table 1.

Zero-point gradient energy, Eg ≈ 10^{26} metric unit energy value order of magnitude					
Monopole mass Mm (kg)	10^{-47}		10^{-11}		
Entity sizes out of zero-point microblackhole (m)		10^{-8}			10^{-26}
Estimated space-time extent		10^{28}		10^{-8}	
Monopole core size (m)			10^{-30}		
Charge of a monopole			1/2e		
Fermion size (m)			10^{-18} to 10^{-15}		
Estimated size of PDP monopole particle circuit assembly (m)			$<10^{-26}$		

VI. OBSERVABLE QUANTUM PHYSICS DISCONTINUITY COMPUTING

The author has shown applying Equation (3) of "stringmetrics" by letting $\tau_{energy}\,\Psi_{fields} = V\,\rho(t)$, reasoned out in earlier publications to arrive to Physics conjecture of "$\tau_{energy}\,\Psi_{fields}$" providing observable. Simple proof analog ρ(t) = energy quantum density form of charge, where i defined as current density, we get result V ρ(t) = V i = power density, δP, This enables author to deduce τ_{energy} to be equivalent to δP. Since energy = $\hbar(\tau)^{-1}$, time differential change in the geometry/topology are inferable by setting {(δP)(geometry)} to be in the form of electrical energy observable in terms of mechanical motor action or photon light action; then, geometry will refer to {area, volume} multiplicative factor to transform power density to energy form. Since mechanical motor action or photon light action are physically

observable, the author can prove "$\tau_{energy}\ \Psi_{fields}$" to be observable parameter. Lemma of this author further interprets observable Physics "$\tau_{energy}\ \Psi_{fields}$" as also representing "discontinuum line" mathematically.
Analog of potential is velocity, v, and that of a wavefunction is trajectory, r(t). The author has shown that equation [61] of gage transform is:

$$g[r_{DEF}(t)] = g[n(t).\ DL] + g[r_g(t)] = g[n(t)].g[DL] + g[r_g(t)] = g[r_g(t) \qquad (7)$$

where g = gage differential, **rDEF(t)** = discontinuum energy field spatial length in time, t, **n(t)** = number discontinuum lengths with time, t, **DL** = discontinuum length, g[DL] = 0 having **DL** = constant, **rg(t)** = gap length of discontinuum length **DL** as a function of time**.** One may envision characterizing discontinuum length DL and the gap length $r_g(t)$ by binary matrix since these variables logically are discrete parameters. $r_g(t)$ is thus quantized codable as 1….0….1….1….0….1, eventually enabling to discretize time space sense.

VII. MACROSCOPIC SIMPLE EXAMPLES OF APPLIED PROBLEM-SOLVING PHYSICS NORMAL OBSERVABLES

The author has already demonstrated earlier with the following situational PHYSICS [61], with:

$$\begin{pmatrix} [\mathbf{Gg}]\,\boldsymbol{\Gamma}^{\mathbf{l}}_{\mathbf{ij}} \\ [\mathbf{Gg}]\,\boldsymbol{\Gamma}^{\boldsymbol{\xi}}_{\mathbf{ij}} \end{pmatrix} \begin{pmatrix} \hat{\boldsymbol{\varepsilon}}_{\mathbf{GR,v}} & \hat{\boldsymbol{\varepsilon}}^{\mathbf{g}}_{\mathbf{GR}} \\ \hat{\boldsymbol{\varepsilon}}_{\mathbf{GR,g}} & \hat{\boldsymbol{\varepsilon}}^{\mathbf{v}}_{\mathbf{GR}} \end{pmatrix}^{-1} (\boldsymbol{\Psi}\mathbf{d1}\ \boldsymbol{\Psi}\mathbf{d2}) \begin{pmatrix} \boldsymbol{\Psi}\mathbf{s1} \\ \boldsymbol{\Psi}\mathbf{s2} \end{pmatrix} \begin{pmatrix} \hat{\boldsymbol{\varepsilon}}_{\mathbf{GR,v}} & \hat{\boldsymbol{\varepsilon}}^{\mathbf{g}}_{\mathbf{GR}} \\ \hat{\boldsymbol{\varepsilon}}_{\mathbf{GR,g}} & \hat{\boldsymbol{\varepsilon}}^{\mathbf{v}}_{\mathbf{GR}} \end{pmatrix} = \begin{pmatrix} \boldsymbol{\Gamma}^{\mathbf{d1}}_{\mathbf{ij}} & \boldsymbol{\Gamma}^{\mathbf{s2}}_{\mathbf{ij}} \\ \boldsymbol{\Gamma}^{\mathbf{s1}}_{\mathbf{ij}} & \boldsymbol{\Gamma}^{\mathbf{d2}}_{\mathbf{ij}} \end{pmatrix} \begin{pmatrix} \hat{\boldsymbol{\varepsilon}}_{\mathbf{GR,v}} & \hat{\boldsymbol{\varepsilon}}^{\mathbf{g}}_{\mathbf{GR}} \\ \hat{\boldsymbol{\varepsilon}}_{\mathbf{GR,g}} & \hat{\boldsymbol{\varepsilon}}^{\mathbf{v}}_{\mathbf{GR}} \end{pmatrix} \mathbf{(8)}$$

where in a lake population pattern of swimming ducks and swans exist, having ducks moving in a row, $\Psi_{\mu} = \Psi_{d} = \Psi_{ducks}$, $\Psi^{\mu} = \Psi^{s} = \Psi^{swans}$, (which are probability functions quantifying population pattern with swans/ducks, observations showing swans move in swimming direction, however, ducks oriented at different directions), ρ_{ds} = density pattern of populated ducks and swans, $[G_g]_{\Gamma ij}$:

the functional, G_g having Γ_{ij}, signal/noise ratio of sound (Γ_{ij}^{ξ}), light(Γ_{ij}^{l}), as well as modon strings {[d]=>::<=[s]} of G_g modulating swans/ducks movements, $\mathcal{E}_{GR} = (\mathcal{E}_{GR})_{gv}$ = gauge fields corresponding to equivalent mechanics: [g, v]{gradient, vortex} with up and down pressure as well as temperature. Thereby, gradient = temperature, pressure = vortex fields, hence observables can be algorithmized as expansion matrix: $<\Psi ducks(tg)| = (\Psi d1\ \Psi d2)$ "ducks on a row";

$|\Psi swans(tg)> = \begin{pmatrix} \Psi s1 \\ \Psi s2 \end{pmatrix}$ "swans on arrow". The gradient fields are up/down temperature, and the vortex fields are anticlockwise-clockwise pressure. Configurations therefore will be:

$[G_g]\,\Gamma_{ij}\ [(\mathcal{E}_{GR})_{gv}]^{-1}(<[\Psi_d(t_g)]|[\Psi^s(t_g)]>)[(\mathcal{E}_{GR})_{gv}] = [\rho_{ds}\ (t_g)]*[(\mathcal{E}_{GR})_{gv}]$. Application of the Equations (4) and (5) give these results. Permutating process population pattern sequel will help to generate simulation algorithmic equation of the moving population greater than [2 × 2] matrix of the above-mentioned example.

1. **Intensity Matrix versus Density Matrix four-vector Formalism Physics:** The author has shown using

Equation (5) with gauge fields [ℰ] ≡ {0, off, on} to be numerical matrix: $\begin{pmatrix} 0 \\ \emptyset \\ 1 \\ \phi \end{pmatrix}$, calibrated as physics procedures standards; here, "0" = zero fields, "∅" = neither off nor on fields, "1" = on fields; "ϕ" = both off and on fields, which would be true in the quantum entangled fields. "∅" = neither off nor on fields are equivalent intermittent nonzero field, switching or flickering observable signals. "ϕ" = both off and on fields would be quantifying quaternionic, turbulent, excessive, or entangled conditional form, encountered for example in explosive situations. Equation (5) transforms to the following [72].

$$(. \Gamma_{\omega,gr} .) =>: :<= \begin{pmatrix} \mathbf{0} \\ \emptyset \\ \mathbf{1} \\ \boldsymbol{\phi} \end{pmatrix} \left(\boldsymbol{\psi c} \,,\ \ \boldsymbol{\psi \jmath} \,,\ \boldsymbol{\psi_+ \psi_-} \right) \textbf{ specific case with } \phi \equiv \textbf{i}. \qquad \textbf{(9)}$$

Methodology: In mathematics, equation (9) represents a four-vector matrix in the form of a 4x4 quaternion matrix. Equation (5) can be applied to 4x4 quaternion wavefunction gaging field physics with micro-macro space, charge, complex, astrophysical, and quantum electromagnetic gravity fields that are entangled, decohered, neither or both wavefunction quaternion forms, and this has the ability to quantify electromagnetic gravity. These are very helpful in moving from particle PHYSICS Standard Model categories to group theory fields groups. Thus, the overall observable parameters that are measurable by observation are as follows: {"G", "M"} = matrices affected by "ρ", and {"Γ" = matrix affected by wavefunctions + gauges fields. "G" = functional "Stringmetrics" field factor, "M" = "Stringmetrics" mass factor, "Γ" = Hod-PDP signal/noise factor, and "ρ" = density factor, providing fields-masses. We see that: $\rho = |\psi\rangle\langle\psi|$.

The author has proposed **Quantization of time** feasible PHYSICS with Corrado Massa's minimal power determinations of 10^{59}ergs/sec giving quantum_time ~ $1/(10^{59}.10^{-7}) \sim 10^{-52}$secs. The author has Table 1 interpretation of quantum monopole to exist below 10^{-52} seconds, further between 10^{-52} seconds and 10^{-34} seconds (Planck_time), entities may be existing as W.I.M.P. dark matter. Above 10^{-34} seconds, entities are likely to exist as quasi-particles like Hod-PDP assembly

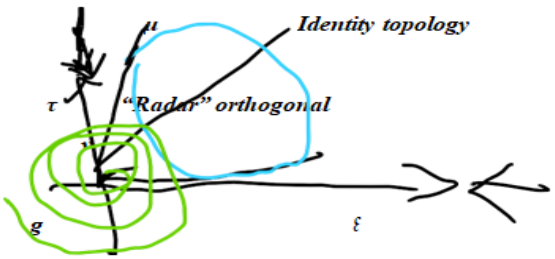

{telemetry} rotational gravitational [70] schema

Mainly there are five fields per Aleksey Zakharenko's PHYSICS that will include two exotic fields with **magnetic, electric, elastic, gravitational, and torsional fields**, possessing five types of universal/local symmetries & waveforms. **(1) Perfect symmetry matrix (2) Time reversal symmetry (3) Magic square symmetry matrix (4) Prime factored symmetry (5) Π symmetry matrix.** The author has graphed schematically with algorithm gage PHYSICS**: x=μ(magnetic), y=ν(electric), X=Ɛ(elastic), Y=τ(torsional), g=gnr=g((gravitational)** to representing **gage algebra:** $(\mathbf{x},\mathbf{y})^{\mathbf{X}}_{\mathbf{Y}}$**to give:** $(\boldsymbol{\mu},\boldsymbol{\nu})^{\boldsymbol{\mathcal{E}}}_{\boldsymbol{\tau}}\big|_{\boldsymbol{\theta\Phi}}\mathbf{g}$, with proposition: Zeroth dimension ≡ absolute vacuum, and **1 to 5** dimensions exhibiting zitterbewegung to alpha information waves!!

Reconstructing the algebraic generalized mediating environment interacting entity using the Feynman diagram quanta flowchart and retrofitting the wavefunction and gage field phase-angle information [84]:

Figure 5: states that if **X =** $\boldsymbol{q_n}$**,** the monopole **N** quantum charge, **Y =** $\boldsymbol{q_s}$, the monopole **S** quantum charge, **Ɛ = QƐ**, the **Q** factor of dipole environment **Ɛ**, then **X' =** $\boldsymbol{q_g}$**, Y' =** $\boldsymbol{q_l}$. They depend on all the following field aspects: wavefunction, gauge field, timeline vs worldline, temperature (heat), and point potential. It is possible to feel, measure, and assess profile density, potential, temperature, signal/noise, elapsing time, wavefunctions, and switch modes experimentally with point-to-point data.

VIII. QUANTUM GRAVITY MODIFIED NEWTONIAN DYNAMICS PHYSICS DISCONTINUUM MODELING

The author has derived formalism quantum gravity PHYSICS, starting with gravitational Galilean Newtonian equation. Force (Fqg) is Gm_1m_2/r^2, gaged to quantum in the following way: $\mathbf{F_{qg} = (G_{qg})^{-1}\ (r_{qg}{}^4)\ (g[r_{qg}])^{-1}\ (Hn')^2\ (g[g[r_{qg}]])\ (g[f^{*'}(Hn)]),}$ where symbols G_{qg}: universal gravitational constant (G) gaged to quantum discontinuum; r_{qg}: discontinuum energy fields (DEF) spatial length connected to discontinuum length (DL) as a function of time (t); as a result, we have $g[r_{qg}]$ = gage of r_{qg}, which is the gage discontinuum quantum velocity corresponding to DEF. Topology, such as rotational or toroidal mobius strip manifold spatial geometry, will be represented by ($r_{qg}4$). ($g[g[r_{qg}]]$) will stand for gage of gage of r_{qg}, which is gage acceleration similar to that of gravity or gage of discontinuum quantum velocity. Hamiltonian is represented by Hn, which finally relates to Iyer Markoulakis Model Formalism. The differential energy Hamiltonian is denoted by Hn'. The gage of the Legendre transform of the (Lagrangian) Hamiltonian DEF is g[f*'(Hn)]. **Point Laplacian Gradient Microblackhole PHYSICS** has been treated to above equation having time evolution Hamiltonian defining microblackhole vortex action to get Laplacian gage solution with $H = \{i\hbar/(t_f\text{-}t_i)\}[\ln|\mathscr{L}p(t)|]$. Substituting this value of Hamiltonian in the above Equation with $H_n = H = \{i\hbar/(t_f\text{-}t_i)\}[\ln|\mathscr{L}p(t)|]$, and differential Hamiltonian $H_{n'} = \partial H/\partial t = (\partial/\partial t)(\{i\hbar/(t_f\text{-}t_i)\}[\ln|\mathscr{L}p(t)|]) = \{i\hbar/(t_f\text{-}t_i)\}\{\mathscr{L}p(t)/\mathscr{L}p(t)\}$, with differential Laplacian $\mathscr{L}p(t)$ to be computed per physics calculus. Hence, algorithmic equation of typical microblackhole gage gravity force [70] (F_{qg}) transforms to:

$Fqg = -i\hbar^3(Gqg(tf-ti)^3)^{-1}\ (rqg^4)\ (g[rqg])^{-1}\ \{\mathcal{L}'p(t)/\mathcal{L}p(t)\}^2\ (g[g[rqg]])\ (g[f^{*'}(\ln|\mathcal{L}p(t)|)])$ (10)

Invoking Operator Algebras, functions, functors, transforms and detailed mathematical physics treatment with more than 20 pages of derivational process, the author has expressed the Equation (10) with only time, space-field, and rotational parameters quantifying essence of the quantum gravity PHYSICS!! With inverse Fourier transform from the time domain to the rotational (frequency, ν) domain, noting the time, $t_g \equiv F^{-1}(\omega)$, and hence, $t_g \equiv F_g^{-1}(\omega)$, the inverse Fourier transform of angular velocity or speed, $\omega = 2\pi\nu$, taking into account Hod-PDP mechanism to have trixial rotational orthogonal contributions like [(ω)] effective =>::<= {θspin, ηrotation, κrevolution}, which are the angle of spin, angle of rotation, and angle of revolution of Hod-PDP quantum assembly explained per published algorithm model ICMHZT.

Figure 4's explanation of Hod-PDP assembly of the rotational fields uses the published algorithm model ICMHZT magneto-electric schematic to illustrate PDP quantum assembly. The resulting algorithm equation, $[Y] = g_g[X]$, has graphical metrics and represents mathematical transformations and operational manipulations carried out entirely with simplifying computing. The output matrix [Y] is a metrically adjusted function of input metrical matrix [X], where g_g is a gage fibrational string parameter. In general, $g_g = 1$ yields an algorithm that results with graphical equation. Scalar quantum gauge field graphic equation $\|[\mathcal{E}_{GR}]\|$ in terms of general transforms with Laplacian, Fourier, and the Legendre gaging the spin, rotation, revolution, and ωqg as a function of time will be such a graphical equation having entirely algebra transform-based theoretical to experimental observable measurable parameters. This extensive mathematical change of the operator algebra has basically eliminated universal constants, which may not be constants over lengthy periods of observations.

IX. ALGORITHM NUMERATION MATRIX SIMULATION PROGRAMMABLE

Equation (10) with above explained methods, the author transformed quite in general to time tensor gauge field rotation, spin, and revolutions only as a function of space-fields-time [83].

$[X] = \{(\mathcal{L}'p(F^{-1}(g[\{\cos\theta spin(t),\ \sin\theta spin(t)\},\ \eta rotation(t),\ \kappa revolution(t)])))^2\ (\mathcal{L}p(F^{-1}(g[\{\cos\theta spin(t),\ \sin\theta spin(t)\},\ \eta rotation(t),\ \kappa revolution(t)])))^{-2}$
$(g\ [f^{*'}(\ln|\mathcal{L}p(F^{-1}(g[\{\cos\theta spin(t),\ \sin\theta spin(t)\},\ \eta rotation(t),\ \kappa revolution(t)]))])\}^{-1}.\omega qg(t)$
$[Y] = \|[\mathcal{E}GR]\|$ **(11)**

where $\mathcal{L}p$: Laplacian; $g[f^{*'}(f'(p^2))] \equiv$ gage of Legendre transforms of Lagrangian energy term p^2/m having p: momentum, and m: mass has been taken care of with transform manipulations.

$\mathcal{L}p(F^{-1}(g[\{\cos\theta_{spin}(t),\ \sin\theta_{spin}(t)\},\ \eta_{rotation}(t),\ \kappa_{revolution}(t)]))$: Laplacian of inverse Fourier gage angular {spin, rotation, revolution} which are functions of time.

$\mathcal{L}'p(F^{-1}(g[\{\cos\theta_{spin}(t),\ \sin\theta_{spin}(t)\},\ \eta_{rotation}(t),\ \kappa_{revolution}(t)]))$: Jacobian, 1st derivative of the Laplacian of the inverse Fourier gage angular {spin, rotation, revolution} as functions of time.

$\omega_{qg}(t)$: quantum gravity angular velocity as a function of time.

$\|[\mathcal{E}_{GR}]\|$: scalar space quantum gauge field matrix protocol, measurable normalized parameter.

1. **Prototype Set-Ups, Figures, Variable Measuring Instrumentation Systems Experimental Designs:** The flowchart in Figure 6 describes the wavefunction-potential inside Superluminous_Plenum with north and south monopoles44 or normally dipoles like Hod-PDP will provide an output signal/noise matrix that is quantum parametrically forked to switching gauge fields and then independently as wave function characteristics: { spin, rotation, revolution} matrix particles that are postulated to emerge from the universal Superluminous-Plenum quagmire as separate wave functions.

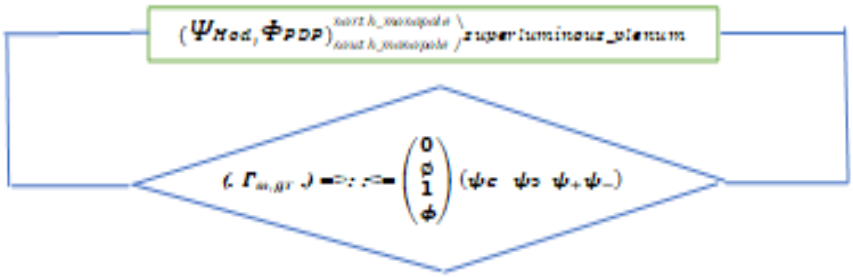

Figure 6: General measurement procedure theoretical to experimental with Algorithm Equations (5) and (9) with explanations giving parametric measurement grid flowchart [83] schematically.

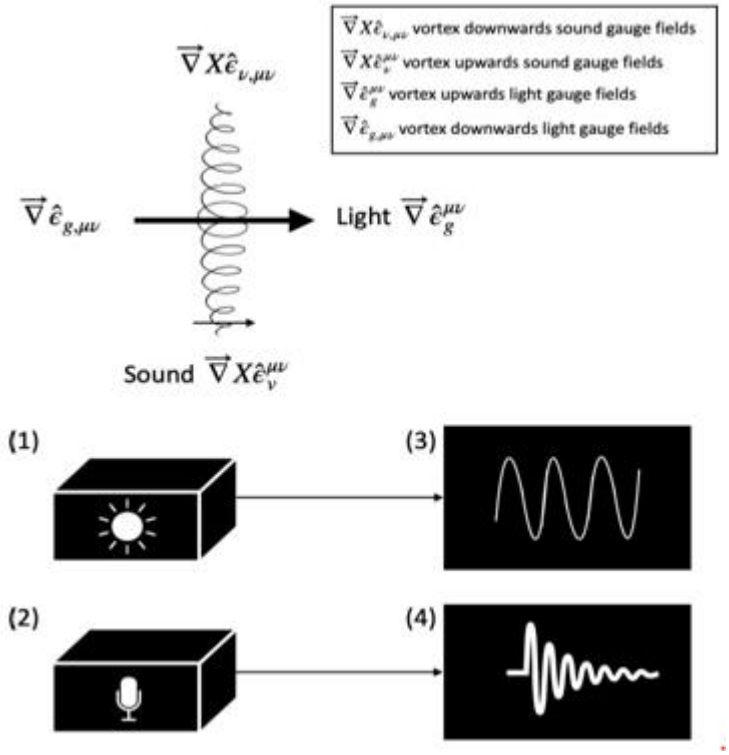

Figure 7: The diagram illustrates an instrumentation system [83] for measuring signal/noise matrices with high precision, incorporating integrated circuit microprocessors and diamond chips. This system can effectively detect and decode observable astrophysical signal/noise matrices related to sound and light using sensors. These decoded signals are then processed by component elements connected to an oscilloscope, spectroscope, and sound meter to

assess various fields and quantify quantum wavefunctions based on Algorithm Equations (5) and (9).

A microprocessor-based operational device with embedded diamond chips is employed for measuring point-to-point astrophysical light intensity, signal-to-noise ratios, and spectral density matrices. (2) The operational device utilizes a piezoelectric acoustic-electric transducer to measure sound profiles, signal patterns, and density matrices, with embedded switches for signal modulation. (3) Photometer sensors with point-to-point profiling capability and switchable modes (0, off, on) are used to measure signal/noise patterns, with the results displayed on an oscilloscope and calibrated for enhanced accuracy. (4) Sound-meter spectroscopic attachments are employed for measuring signal/noise patterns, and the data is displayed on an oscilloscope and subjected to calibration for improved precision. In summary, the Poynting vector can be applied to assess the electric and magnetic fields of light at a specific location using the formula S = (E x B) / μ0.

The Figure 7 method offers a practical way to capture observable and measurable astrophysical signal/noise matrices related to sound and light. These parametric scalar gauge fields are then appropriately transmitted to sensors that are connected to oscilloscope, spectroscope, and sound meter measurement systems. These sensors are specialized devices equipped with integrated circuit microprocessors and diamond chips, ensuring precise point-to-point detection of astrophysical light intensity signal/noise and spectra density matrices. Additionally, photometer sensors with point-to-point profiling switches in modes {0, off, on} are utilized to measure signal/noise pattern density matrices with enhanced calibration systems. Sound signals are also captured separately, sent to detectors, and analyzed using acoustic-electric transducer profile switches to measure signal pattern density matrices.

X. FIBRATIONAL BUNDLE GAGE TRANSFORMS PHYSICS SYSTEMS

Algorithmic Graph Equation (11) in fibrational graphic form of $\mathbf{[Y] = g_{fts}\,[X]}$ can be substituted to gage specific parameters as $\mathbf{||[\mathfrak{C}_{GR}]|| = g_{fts}\ f(grouping\_transforms(time)).}$ Mathematically inverse operation of this equation gives algorithm: $\mathbf{grouping\_transforms\ (time) = f^{-1}(|||[\mathfrak{C}_{GR}]||/g_{fts}).}$ Time is mathematically inverse transform, giving four-vector time matrix [72]:

$$||\begin{pmatrix} \hat{\mathbf{t}}_{\mathbf{pr},\mu\nu} & \hat{\mathbf{t}}_{\mathbf{g}}^{\mu\nu} \\ \hat{\mathbf{t}}_{\mathbf{l},\mu\nu} & \hat{\mathbf{t}}_{\mathbf{r}}^{\mu\nu} \end{pmatrix}|| = \mathbf{g^{-1}[f^{-1}(|||[\mathfrak{C}_{GR}]||/g_{fts})] = g_{ifts}\,[transforms]} \qquad \mathbf{(12)}$$

where with $\hat{t}_{pr,\mu\nu}$:proper time, $\hat{t}_{r}^{\mu\nu}$: real time, $\hat{t}_{g}^{\mu\nu}$: global time, and $\hat{t}_{l,\mu\nu}$: locally time; $||[\mathfrak{C}_{GR}]||$: scalar space gauge matrix fields gaging to normalized four-vector time matrix.

XI. QUANTIFICATIONS, MEASUREMENTS, AND DISCONTINUUM GRAVITY_BUNDLE_TRANSFORM PHYSICS

The author has derived the following equation based on peer published articles Discontinuum PHYSICS that Taylor and Iyer have generalized embodied-energy-discontinuum (EED) field and a disembodied-energy-discontinuum (DED) field to be a part of each other. **Gist of what it will apply to quantify discontinuum PHYSICS** with a

simpler way uses the formalisms, applying results of Equations (11) and (12) to obtain algorithmic equation expressing [72]:

(DEF) = (gravity_bundle_transform) (weight) = Σ{(fiber_transforms)*(gage_velocity)} **(13)**

having **DEF = spatial differential of gravitational force = ∂/∂r(GmM/r^2)** and **M/r^2 = ρr^3/r^2** such that **ρ** = gravity density matrix that is equivalent to concentrated huge gravitational mass, **M** which is having its gravitational influence spreading over **r**, the spatial distance between **m** and **M.** Equation (13) summarizes with a gist of DisContinuum PHYSICS (DCP), allowing evaluation of the Discontinuum_Energy_Field (DEF) by having computation of algorithm using typically algebraically general mathematics: [Y] = f_T [X], defining $f_T \equiv$ fiber_transform, having gage_time with gage_fields of light and sound that can be connected to Taylor and Iyer TOR predictions with the discontinuum physics so that gage_velocity will correlate with that discontiunnum object equation of motion. Experimental observations with measurements of gage_velocity and the weight relationships to facilitate an experimental design by having circuit analog will be made feasible via theory simulating Equation (13). In the above relation [Y] = f_T [X], [Y] and [X] have parametric adjustments to estimate (DEF). Algorithm Equation (13) tells us that determination of the (gravity_bundle_transform) is possible by having programmatic computation of general equation of the algorithm [Σ{(fiber_transforms)*(gage_velocity)}]/(weight). Therefore, DisContinuum Physics gage unifies paradigm shifting PHYSICS.

XII. IT OF ALGORITHM QUANTUM COMPUTING PHYSICS CODING MATRIX

The author has simplified Equation (9) into compact algorithm IT coded to represent states of time switching quaternion patterns with states of switch off = 0, on =1, not_off = ~~0~~, not_on = ~~1~~ **(note: not_off ≠ on and not_off ≠ off** in general**) operated by "ketvector" [on off]** to generate global and local quantum parameters, $\mathbf{q_g}$ and $\mathbf{q_l}$ is given by $\begin{pmatrix} 0 & 1 \\ \sout{1} & \sout{0} \end{pmatrix}\begin{pmatrix} \text{on} \\ \text{off} \end{pmatrix} = \begin{pmatrix} q_g \\ q_l \end{pmatrix}$ evaluating with Pauli matrices equivalently employing quaternion spinor to get [84]:

$$\begin{pmatrix} \mathbf{0} & \mathbf{1} \\ \sout{\mathbf{1}} & \sout{\mathbf{0}} \end{pmatrix}\begin{pmatrix} \mathbf{on} \\ \mathbf{off} \end{pmatrix} = \begin{pmatrix} \mathbf{0} & \mathbf{-i} \\ \sout{\mathbf{i}} & \sout{\mathbf{0}} \end{pmatrix}\begin{pmatrix} \mathbf{on} \\ \mathbf{off} \end{pmatrix} \quad \textbf{(14)}$$

The author then carried out further analytical mathematics to find the relationship of switching states and off and on modes. Evaluating Equation (14):

0*on + 1*off + ~~1~~*on + ~~0~~*off = -i*off + i*on. Hence**, -i*off + i*on = ~~1~~*on + ~~0~~*off.** Inputting values **~~0~~≡off-on & ~~1~~≡on-off,** we get**: -i*off + i*on = on-off * on + off-on * off.** On simplifying the author gets resultant**: (i – on-off) * on = (i + off-on + 1)* off.** So, off = f(on mode).

$$\textbf{i.e., Off} = \frac{(\mathbf{i - on - off})}{(\mathbf{i + off - on + 1})}\mathbf{*on} \qquad \textbf{(15)}$$

which has a nonzero denominator; an inference will be: if off is nonzero, it's noisy like nebulae!! We can have condition**: off = 0 if i = on-off,** or **(on-off)^2 = -1,** translating to quaternion**s** equation **(on-off)^4= 1.** It will then be analogous to switches mode multiplier, that appears like **"IIQuaternion switches modulating equivalent synthesis waveforms"**. This

can be graphically shown having a square wave that is on-off multiplying over to generate photomultiplier like effects that are shown graphically below.

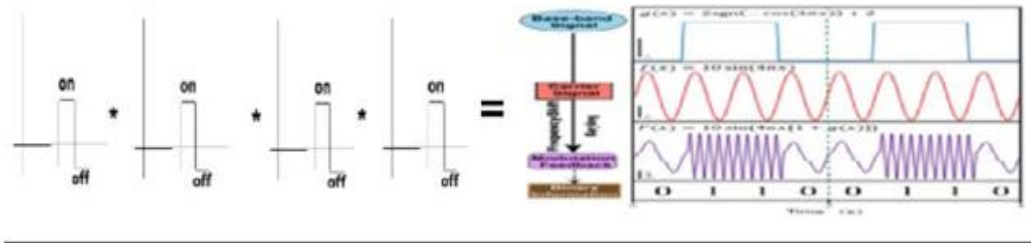

Figure 8: Quaternion on-off switches modulating square waves effect like photomultipliers lasering!! Mesoscopic observable twinkling stars sky!!
[Reference: image Wikipedia output].

There are pattern binary coding sequences that are eventually computer simulatively programmable to show switching signal/noise effects. We can apply Equation (15) to transform Equation (14) into numerical values with binary coding 0 and 1 matrix forms. However, it is to be noted Algorithm IT Quaternions PHYSICS Matrix: $\begin{pmatrix} \mathbf{0} & \mathbf{1} \\ \mathbf{\cancel{1}} & \mathbf{\cancel{0}} \end{pmatrix}\begin{pmatrix} \boldsymbol{on} \\ \boldsymbol{off} \end{pmatrix} = \begin{pmatrix} \boldsymbol{q_g} \\ \boldsymbol{q_l} \end{pmatrix}$ has non-integer values with $\cancel{0}$ and $\cancel{1}$. In the following, the author has derived equivalent numerical matrix by recognizing the natural processes of the prime number factorizations. Hence, $\mathbf{\cancel{0}}$ **= pf0** and $\mathbf{\cancel{1}}$ **= pf1** in notation symbols to programming.

XIII. PHYSICS RESULTS MATRIX VALUE CODING

$\begin{pmatrix} \mathbf{0} & \mathbf{1} \\ \mathbf{\cancel{1}} & \mathbf{\cancel{0}} \end{pmatrix}\begin{pmatrix} \mathbf{on} \\ \mathbf{off} \end{pmatrix} = \begin{pmatrix} \mathbf{q_g} \\ \mathbf{q_l} \end{pmatrix}$ the logic Algorithm IT Quaternions PHYSICS Matrix will become [84]:

$$\begin{pmatrix} \mathbf{0} & \mathbf{1} \\ \mathbf{pf1} & \mathbf{pf0} \end{pmatrix}\begin{pmatrix} \mathbf{1} \\ \mathbf{0} \end{pmatrix} = \begin{pmatrix} \mathbf{q_g} \\ \mathbf{q_l} \end{pmatrix} \qquad \textbf{(16)}$$

Equation (16) has parameters **pf1** (permutating) as taking up values of (1/prime_number); thereby, **pf0** (permutating) taking up conjugatively values (-1/prime_number); we know already, [prime_number] set takes values of {1, 2, 3, 5, 7, ……} input to syntactically machine coding computer program. Graphically then plotting **[X] axis = $\mathbf{q_g}$:** the quantum global versus the **[Y] axis = $\mathbf{q_l}$**: the quantum local parametric values will output PHYSICS characterizing properties!! Typical examples with arithmetic numeration matrix calculations are given in many of the author's peer publications with computer programming simulation graphing providing generated results also demonstrated earlier in this Chapter.

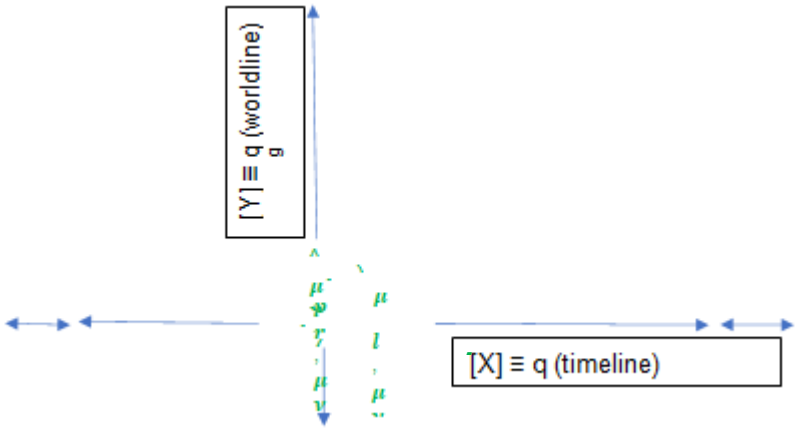

Figure 9: tensor time four-vector matrix rotated to correspond to graphing quantum parameters variables with [X] ≡ q$_l$(timeline) and [Y] ≡ q$_g$(worldline) axes Equations (11) through (16). Graphing the global quantum, q_g, versus the local quantum, , by rotation matrix to suit **[X]-[Y]**, which are interchangeable, plotting corresponding to tensor time four-vector matrix format in this figure [84].

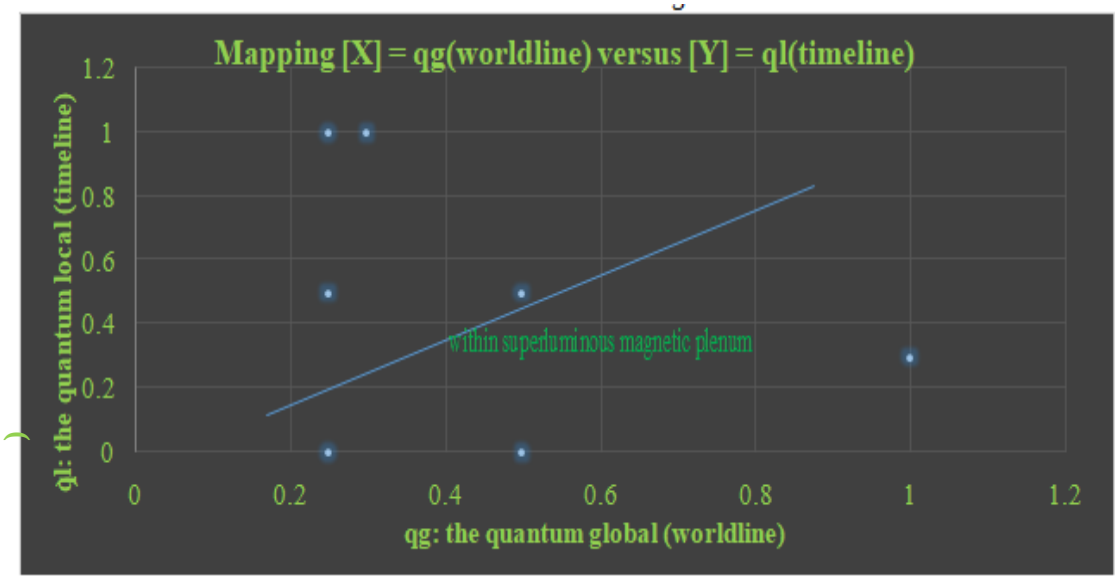

Figure 10: schematically shows mapping [X] = (worldline) versus [Y] = q_l(timeline). Where [X] and [Y] are adjusted to PHYSICS operator metrix protocol, plotting quantum probability values manifesting Equations (15) and (16), within Superluminous Magnetic Plenum [84].

Here, briefly these preliminary theoretical results are enumerated executing program to compute q_g and q_l for **pf0** and **pf1** prime numbers up to 10,000 in one case and 100,00 in the other. [84] **Figure 11** shows results.

1. Results for 10,000 prime number factorisations* (M1)

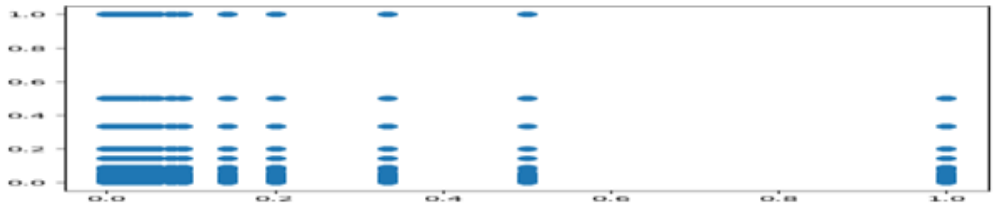

2. Results for 100,000 prime number factorisations* (M2)

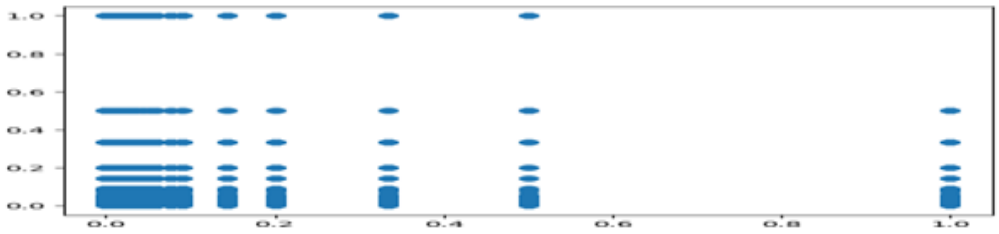

^Origin (0, 0) zero time point ^(vacuum?!) intersection nodes of timeline weaving worldline!! Figure 11: generates a graph [84] to display a computer-programmed equation (8) to map q_l and $q_g$for prime numbers of pf0 and pf1 up to 10,000 in case (M1) and 100,00 in case (M2). pf1 (permutating) = 1/prime_number; pf0 (permutating) = -1/prime_number is the mathematics constraint with [X] axis = q_l: the quantum local; [Y] axis = q_g: the quantum global parametrizing variables. Courtesy: Christopher O'Neill, IT Physicist of Cataphysics Group, Ireland coding* as well as executing computer simulation programming**.**

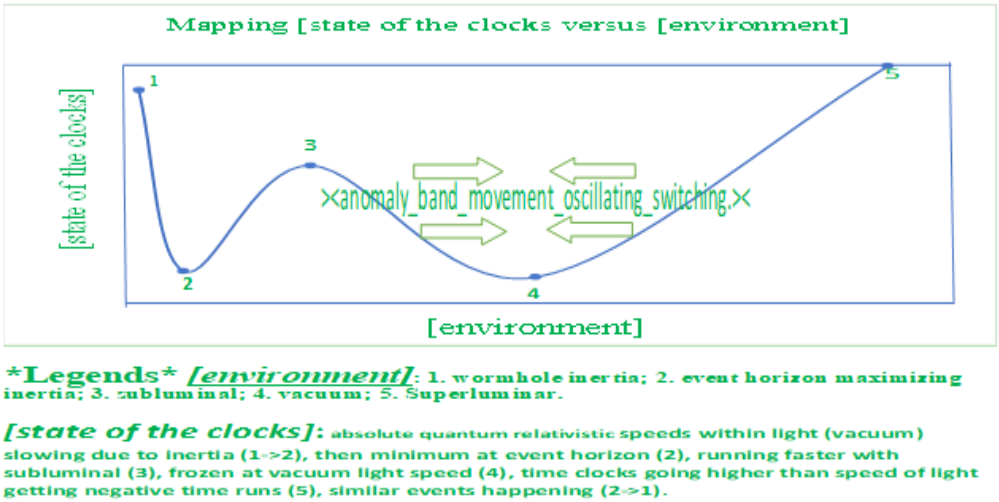

Figure 12: The clocks' current status in relation to the environment's interaction (schematic outlines) [84]. Legends describe how the environment, in particular in a quantum relativistic sense, impacts the status of the clocks. Superimposition of analog clock on mapping [state of the clocks] versus [environment] we get time core information-time comparing quantum

global mapping quantum local. One may surmise: environmental point ><1>< <-> ><5>< may represent conscious mind, point ><1,2><3>< <-> ><4,5><3>< may represent subconscious mind, point ><2>< <-> ><4>< may represent unconscious mind existing in environment!!

XIV. ANALYSIS OF SWITCHES STATES EQUATIONS (14)&(15) QUATERNION MATRIX

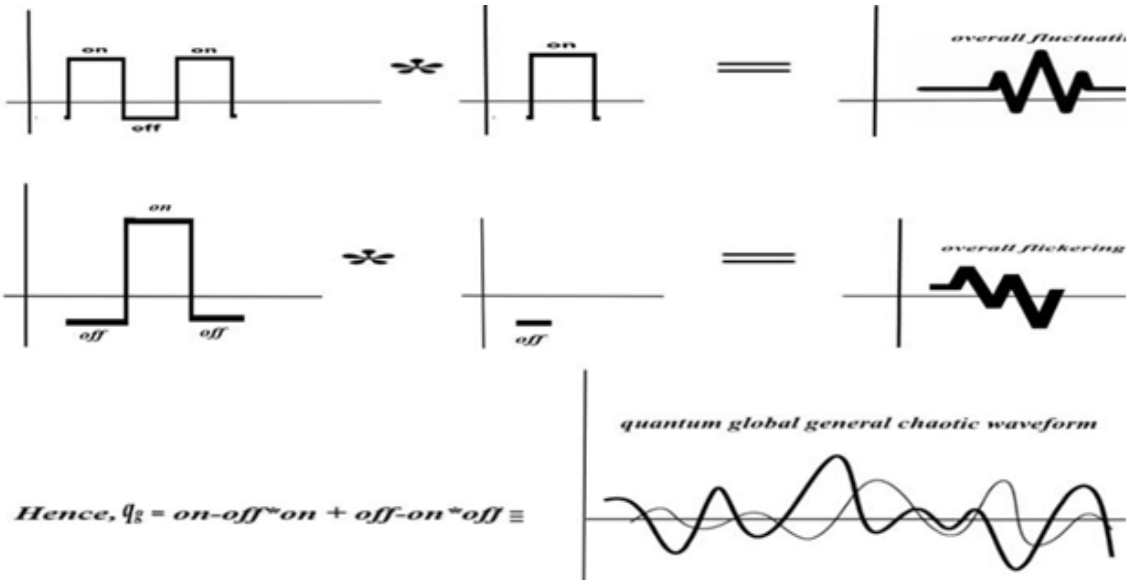

Figure 13: The graphical solutions to Equations (14) and (15) having q_g = on-off*on + off-on*off to give prime number values: pf1 = ~~1~~ = on-off, pf0 = ~~0~~ = off-on, refer to the main text as well. Keynote: scalar space gauge field can also be written in square bracket notation like: [0 off-on 1 on-off] switching analog form to indicate mode of switches, with 0 indicating no switches or vacuum; off-on indicating mostly off-mode but coming on or flickering; 1 indicating mode on condition switches; on- off indicating mostly on but mode coming off or fluctuating [CJPAS, Vol. 17, No. 3, pp.5745-5760, October 2023 Appendix II].

Geometry of space From dimensional {Hod, dipole, magnetic, planar field} to dimensionless {point, Superluminous, Plenum, magnetic, quagmire}, {PDP, clockwork, assembly, discontinuum, mechanism} to {particle, photon, quark, gluonical, matter}. The process of creating a Hod-dipolar planar magnetic rigid entity with high energies to break symmetry and create quasi-particles that generate electron-positron pairs to assemble with north-south monopoles to create a PDP circuit clockwork mechanism is graphically represented by a flowchart similar to the Feynman diagram (Figure 14). The quark-gluonical particle is possibly induced to matter-forming by the Hod-PDP assembly via photon wave (generated by Hod) mediation. The procedure is illustrated graphically below**.** Hod_Plenum mechanism is the key PHYSICS for the author's collaborative coauthor John Hodge's Scalar Theory of Everything.

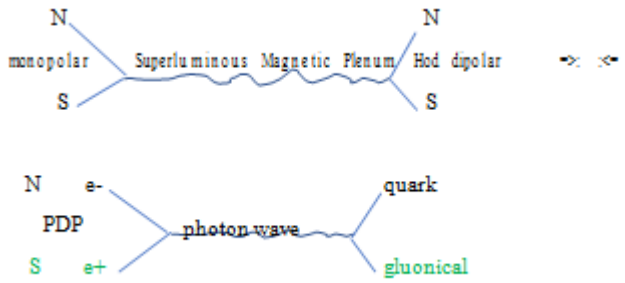

Figure 14: Two Feynman-like diagrams. One showing monopolar to Hod-dipolar. The other showing PDP to gluonical quark particle [84 Appendix II Fig. II.1].

XV. DIMENSIONAL CONJECTURAL PHYSICS SHIFTING PARADIGM

Essentially, we can validate the physics hypotheses by providing evidence for the sizes of the different components of the universe, which are enumerated in Table 2 for your convenience.

Table 2: The object and anticipated characteristic across many dimensional spaces. Probabilistically, adsorption signals can happen with both Hod and Hod-PDP clocking systems [84 Appendix II Table II.1].

Dimensional range	Entity and expected property
0 to 1	Superluminous Plenum that may be noisy, however not observable
1 to 2	Open strings, typically 1D; Closed strings or loops, typically 1D to 2D
2	Hod that will not have thickness, hence transparent not observable
2 to 3	Quasi-particles, particles like fermions and bosons - potentially observable
3	Matter universe general Euclidean observable
3 to 4	Space-time manifold, for instance, blackholes observable effects
4 to 5	Hod-PDP assembly dynamics, effects quantum physically interpretable

We can sketch time-event connecting sense rotations with geometry of space per **Figure 15.** Sense space

Figure 15: The diagram for time-event connecting sense to space [84 Appendix II Fig. II.2].

XVI. THEORETICAL ALGORITHM GRAPHING WAVE PARTICLE REAL LINK VALUE

Now, let's analyze the diagram depicted in Figure 5. Within this figure, Ψ represents the wavefunction of the electron-positron pair, while φ denotes the gauge field function with a phase angle that can be determined through experimental measurements presented in Figures 6 and 7. Consequently, the values of (ψ, φ) can be calculated to achieve a comprehensive quantification of the process diagram described [84 Appendix II Fig. II.3]:

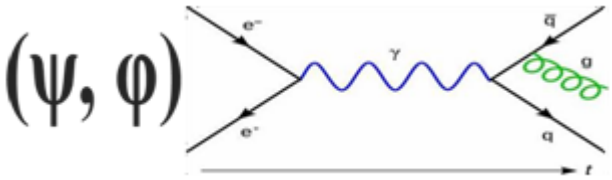

Figure 16: The Feynman-like diagram of electron-positron mediated by light photon to generate quark, antiquark, as well as gluon in the time scale. The retrofitting of this diagram upfront with the wave function and phase angle per Figure 5 scheme will help to establish particle quantum conditions. This algorithm, combined with ITSTEM physics, will serve various purposes, particularly in the realm of quantum computing applications. The complete system, encompassing software algorithms and hardware particles, will contribute to the stability and self-correction of quantum computer equipment. It will also facilitate the operational calibration of accessories that may be provided in conjunction with the future quantum computer having internet technology enhanced operating systems.

XVII. STRONG GRAVITY VERSUS WEAK GRAVITY THESIS PHYSICS

1. Weak gravity will act like stranded (open) or thread tugging, however strong gravity will act like a rope, which is a braided (closed) bundle of strings system able to pull enormous weight. Strong gravity is similar to a closed braided bundle system of strings that pulls heavy objects toward the center of gravitational mass by functioning as a single unit system pulled by stress tensor towards the center of gravitational mass.

2. A horizontal force known as weak gravity can be seen on the tangential plane of a stratified geodesic, such as the Earth, with a spherical concentric equidensity-matrix that is roughly spherical and stratified towards the mass center like a sphere. This pressure increases (and therefore the density matrix) towards the gravity center. Weak gravity will model as fiber transform (open) strings drawing an object. Strong gravity is similar to acceleration caused by gravity, while weak gravity is similar to normal acceleration.

3. Gauge velocity connects strong and weak gravity. Therefore, the equivalency concept connecting weak gravity and strong gravity will apply. Strong gravity is linked by a gravitational acceleration, but weak gravity is typically accompanied having a conjugate acceleration.

4. The matter-energy field of quantum density disperses the influence of an object on its surroundings to nearly infinite extent. High-density fields of strong gravity cause warping, which eventually leads to that causality which curves space-time's geometry to

form objects like black holes. Strong gravity worldline carrier waves are interwoven with a weak gravity timeline. Earth is impacted by the worldline's curvature and the events that occur in it.

5. The weak gravity particle-particle collision interaction of the object's density fields influences environmentally apart objects that causes chain reaction of naturally occurring action and reaction processes simultaneously.

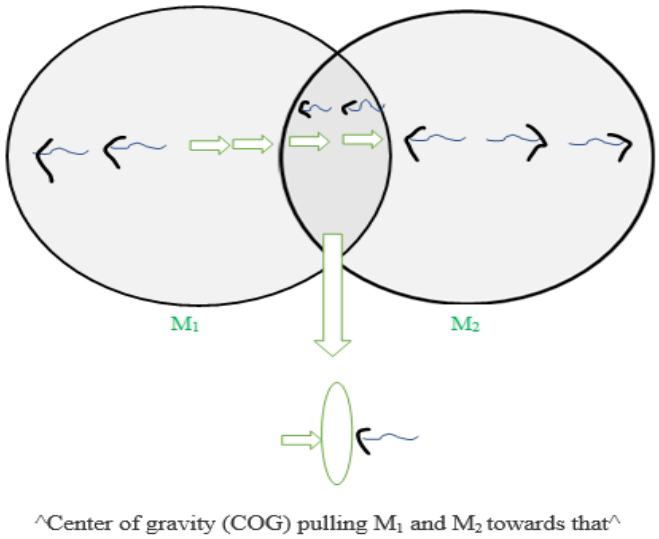

Figure 17: Spreading of density matrix from M_1 and M_2 massive objects pulling towards center of gravity (COG) [85].

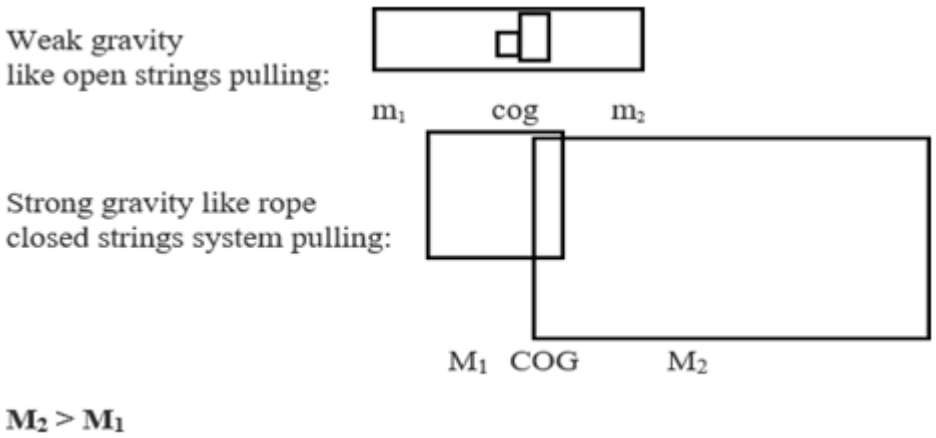

Figure 18: The matter masses m1 and m2 are like open strings pulling on each other, representing weak gravity. Matter masses M_1 and M_2, with $M_2 > M_1$ are like rope constituting braided bundle of the strings together, pulling on each other acting like closed strings system of strong gravity [85].

XVIII. EXPLAINING INTERPRETATIONS PHYSICS DISCUSSING PROPOSITIONS

Figure 17 illustrates how mass is dispersed by matter to generate a distributed density matrix in space. After then, every object will interact with density matrix within its own sphere of influence, attracting or repelling other objects to occupy the same place. Since non-bosonic, or non-light, matter cannot overlap its spatial occupying, any particle, like fermions, that occupies a point in space would displace any other particle that tries to occupy the same space. This will produce a center of gravity (COG) through the action-reaction sequence of collisions, similar to the thermodynamics of perfect gas particles. Although the equilibrium of motion vectors culminates in intersecting regions that balance opposing vectors, this interaction junction of the two objects' spheres of influence is represented as a lenticular region. Using this technique, we may infer that lighter objects with smaller density matrices would usually have weaker spheres of effect compared to enormous objects with larger density matrices. When opposing vectors cancel each other out, there will be a dragging towards COG. Keep in mind that the true vector alignment is not shown with the schematics. Nonetheless, the translational characteristic of vectors will suggest balance in the density matrix vector forces. Figure 18 illustrates how different forces acting on COG might produce strong vs weak gravity. One can test the ability of a single strand of string to pull an object—it can only pull weakly—to illustrate simple weak gravity. On the other hand, strong gravity acts like several strings braided into a rope that can pull quite strongly. Strong gravity acts in this way like tightly wound threads that are difficult to break or extend. The way weak gravity operates can be compared to open strings that are more easily broken or stretched out at the ends.

XIX. ACTION OF STRONG GRAVITY VERSUS WEAK GRAVITY TRANSFORMS

1. At quantum levels strong/weak gravity operator predominates.
2. Strong gravity predominates at astrophysical level.
3. Weak gravity predominates at mesoscopic level.
4. Gravity-time-event mesoscopically interactively couples to energy matter environment.
5. Possibility of wormholes happen at astrophysical short circuiting to quantum level.

XX. QUESTION OF TRUE OR FALSE VACUUM, WEAK, AND THE STRONG ENERGY

Per Figure 12, quaternion switch state on/off will provide knowledge of state of the clock indicating energy minima or maxima. Quantum field theory posits two energy minima of false and true vacuum. It is possible to conjecture false vacuum to be minimum energy with higher absolute temperature, versus true vacuum minimum entropy with lower absolute temperature. {Hadrons, mesons} (2 quarks) gluonic bosons constitute typically higher temperature phases occupying false vacuum. {Hadrons, baryons} (3 quarks) such as gravitonic fermions constitute typically lower temperature phases with true vacuum. Vacuum oscillations possibly extending to the true vacuum from false vacuum, barrier between them might have time space oscillatory characteristics, generating super crystal defects. Possibilities arise having Casimir effect {altering the vacuum expectation value of the energy of the second-quantized electromagnetic fields}in submicron range, i.e., micron to nanometer [https://physicsworld.com/a/the-casimir-effect-a-force-from-nothing/]. Whereas capillary

action can occur at mesoscopic level of 200 microns to meters [https://en.wikipedia.org/wiki/Capillary_action], quantum tunneling occurs at nanometer level [https://phys.libretexts.org/Bookshelves/University_Physics/Book%3A_ University_ Physics_ (OpenStax)/University_Physics_III Optics_and_Modern_Physics_ (OpenStax)/07%3A_Quantu m_Mechanics/7.07%3A_Quantum_Tunneling_of_Particles_ through_Potential_Barriers]. At quantum to subquantum levels, like with Hod-PDP mechanism and Planck processes, vortex and the gradient gauge fields of Helmholtz decomposed point matrix fields {PHYSICS FORMALISMS originated per Iyer Markoulakis approach} may play key role in the vacuum energy phases. With these mesoscopic to quantum mechanisms, we conjecture that minimum energy of higher temperature phase may have vortex fields that capably generate vacuum loops, having speed of light propagation consistent with quantum field theory predictions of vacuum bubbles expanding onto the universal level. Additionally, at the minimum entropy of lower temperature phase, it may have gauge gradient fields that constitute typically fermionic or baryonic oscillations, which has been explained earlier. Microblackholes or blackholes may correspond to the former with vortex gauge fields, while zero-point may correspond to the latter with gradient gauge fields!! False vacuum may thereby constitute microblackholes while true vacuum may constitute zero-point states. Thus synthesis process may create feasibly energetically favorable nucleus originating out of microblackhole within decay of false vacuum states, while electrons pop up at zero-point true vacuum states creating matter from generation of hydrogen atoms multiplicity isotopes to initiate fusion reactions processes within galactical stars operationally!!

XXI. HOW BARYONS, GRAVITONS, AND GLUON QUARK MESONS SYNTHESIZE

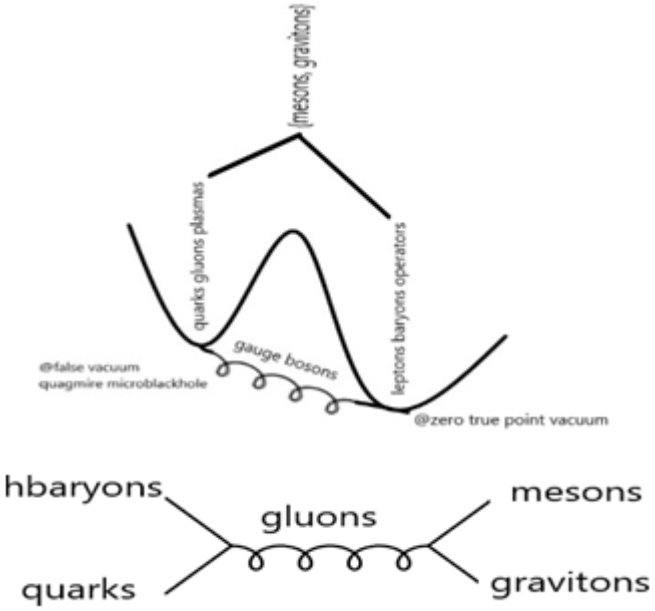

Figure 21: Schematics showing synthesis {weak, strong} system generating particle spectra producing {mesons, gravitons} out of {quarks, gluons} plasmas at the false vacuum quagmire microblackhole (fvqm). Mediating environment gauge bosons combine {leptons, baryons} operators at zero true point vacuum (ztpv). Gage unifying original Iyer Markoulakis

point PHYSICS with Standard Model's mathematical quantum field theory unifies weak and strong fields of nuclear with gravitational gravitons to electromagnetic leptonic fermionic fields. The author's viewpoint graphics bring out the probable possible gage unified symmetry gauge fields.

The true vacuum may act as receptacle to constitute leptons, baryons operating fields within zero point decomposed Helmholtz quagmire, while the false vacuum may act like crucible synthesising the strong interactions of quarks, gluons, plasmas activating in the presence of the gauge bosons. These are systemically feasible if there are microwormholes linking false vacuum microblackholes with true zero pathway point vacuum. They resultantly generate gravitons, mesons radiating emanating from such configurations within sense-time-space manifolds!! All these are brought out in the schematics above of how they come together and how the Feynmann diagrm may be sketched to show the synthesis proceses to foster future PHYSICS project!! Micro macro connection of quantum level processes to astrophysical gaging is made possible with this PHYSICS paradigm!!

XXII. LITERATURE REFERENCES SOURCES

[1] L. F. Wei, Gauge, canonical and Galilean transformations and the non-uniqueness of Lagrange functions, European Journal of Physics, 2020, iopscience.iop.org.
[2] E. Verlinde, On the origin of gravity and the laws of Newton, Journal of High Energy Physics, 2011, Springer.
[3] S. Hossenfelder, Covariant version of Verlinde's emergent gravity, Physical Review D, 2017, APS
[4] L. Randall and R. Sundrum, An alternative to compactification, Physical Review Letters, 1999, APS. E. Noether and N. Jacobson, Gesammelte Abhandlungen-Collected Papers, AMC, 1983, maa.org.
[5] M. A. Tavel: Milestones in mathematical physics Noether's theorem, Transport Theory and Statistical Physics, 1971, Taylor & Francis.
[6] W. Pauli and C. P. Enz: Thermodynamics and the kinetic theory of gases, 2000, books.google.com. V. V. Borisov, A. B. Utkin Some solutions of the wave and Maxwell's equations, Journal of Mathematical Physics, 1994, aip.scitation.org.
[7] S. Hossenfelder and T. Palmer, Rethinking superdeterminism, Frontiers in Physics, 2020, frontiersin.org.
[8] A. Plotnitsky, A. Plotnitsky: Bohr, Heisenberg, Schrödinger, and the principles of quantum mechanics, Principles of Quantum Theory, From Planck's …, 2016, Springer.
[9] Physics: Maxwell's Equations, Light and the Electromagnetic Spectrum. https://www.encyclopedia.com/science/science-magazines/physics-maxwells-equations-light-and-electromagnetic-spectrum.
[10] A. Bohr, B. R. Mottelson, and O. Ulfbeck: The principle underlying quantum mechanics Foundations of Physics, 2004, Springer.
[11] Atom - Bohr's Shell Model | Britannica. https://www.britannica.com/science/atom/Bohrs-shell-model.
[12] W. Pauli: Exclusion principle and quantum mechanics- Writings on physics and philosophy, 1994, Springer.
[13] J. Oppenheim and S. Wehner, The uncertainty principle determines the nonlocality of quantum mechanics, Science, 2010, science.org.
[14] General Relativity, University of Pittsburgh, https://sites.pitt.edu/~jdnorton/teaching/HPS_0410/chapters/general_relativity.
[15] R. Carballo-Rubio, F. Di Filippo, S. Liberati, and M. Visser, Phenomenological aspects of black holes beyond general relativity, Physical Review D, 2018, APS.
[16] O. Dreyer, B. Kelly, B. Krishnan, and L. S. Finn et al., Black-hole spectroscopy: testing general relativity through gravitational-wave observations, Classical and Quantum Gravity, 21, 4, 787-803, 2004, iopscience.iop.org.
[17] S. Hossenfelder: Existential Physics: A Scientist's Guide to Life's Biggest Questions, 2022, Atlantic Books.
[18] First Image of a Black Hole | NASA Solar System Exploration, https://solarsystem.nasa.gov/resources/2319/first-image-of-a-black-hole.
[19] I. Sakalli and A. Ovgun, Hawking radiation and deflection of light from Rindler modified Schwarzschild

black hole, Europhysics Letters, 2017, iopscience.iop.org.
[20] V. Berezin, Quantum black hole model and Hawking's radiation, Physical Review D, 1997, APS.
[21] S. Hossenfelder, A possibility to solve the problems with quantizing gravity, Physics Letters B, 2013, Elsevier.
[22] K. Akiyama et al., First Sagittarius A* Event Horizon Telescope Results. II. EHT and Multiwavelength Observations, Data Processing, and Calibration, Event Horizon Telescope Collaboration, The Astrophysical Journal Letters, Volume 930, Issue 2, id. L13, 31 pp., 2022, iopscience.iop.org.
[23] A. Rueda and B. Haisch, Gravity and the quantum vacuum inertia hypothesis, Annalen der Physik, 2005, Wiley Online Library.
[24] H. E. Puthoff and S. R. Little, Engineering the zero-point field and polarizable vacuum for interstellar flight, arXiv preprint arXiv:1012.5264, 2010, arxiv.org.
[25] S. Hossenfelder: Experimental search for quantum gravity, 2017, books.google.com.
[26] J. F. Woodward, Gravity, inertia, and quantum vacuum zero point fields, Foundations of Physics, 2001, Springer.
[27] S. Hossenfelder, D. J. Schwarz, and W. Greiner, Particle production in time-dependent gravitational fields: the expanding mass shell, Classical and Quantum Gravity, Volume 20, Number 11, 2003, iopscience.iop.org.
[28] S. Hossenfelder, Observables of Quantum Gravity at the LHC, 2007, pos.sissa.it.
[29] L. Randall and M. D. Schwartz, Quantum field theory and unification in AdS5, Journal of High Energy Physics, 2001, iopscience.iop.org
[30] R. L. Jaffe, Casimir effect and the quantum vacuum, Physical review D, 2005, APS.
[31] D. A. Abbott, B. R. Davis, N. J. Phillips, L. Le Su, and K. Eshraghian, Quantum vacuum fluctuations, zero point energy and the question of observable noise, in Unsolved Problems of Noise, eds • Published 1997.
[32] V. L. Ginzburg: Theoretical physics and astrophysics, 2013, books.google.com.
[33] Lisa Randall, Higgs Discovery: The Power of Empty Space, 2013, Harper Collins Publishers, New York, NY, ISBN 978-0-06-230047-8.
[34] R. C. Fernow: Introduction to experimental particle physics, 1986, library.oapen.org.
[35] S. Tavernier: Experimental techniques in nuclear and particle physics, 2010, library.oapen.org.
[36] Manuel Malaver, Hamed Kasmaei, and Rajan Iyer. Magnetars and Stellar Objects: Applications in Astrophysics, Eliva Press Global Ltd., Moldova, Europe, 2022, pp. 274, ISBN:978-99949-8-246-2.
[37] H. Fritzsch, G. Mandelbaum, Weak interactions as manifestations of the substructure of leptons and quarks, Physics Letters B, 1981, Elsevier.
[38] R. Raitio, A model of lepton and quark structure, Physica Scripta, 1980, iopscience.iop.org.
[39] S. Hossenfelder, Theory and phenomenology of space-time defects, Advances in High Energy Physics, 2014, hindawi.com.
[40] A. Salam, J. C. Ward, Electromagnetic and weak interactions, Physics Letters, 1964, apps.dtic.mil.
[41] M. K. Gaillard, P. D. Grannis, F. J. Sciulli, The standard model of particle physics, Reviews of Modern Physics, 1999, APS.
[42] E. Goldfain, Complexity in quantum field theory and physics beyond the standard model, Chaos, Solitons & Fractals, 2006, Elsevier.
[43] L. F. Abbott and E. Farhi, Are the weak interactions strong?, Physics Letters B, 1981, Elsevier.
[44] A. Joyce, B. Jain, J. Khoury, and M. Trodden, Beyond the cosmological standard model, Physics Reports, 2015, Elsevier.
[45] T.P. Cheng and L.F. Li: Gauge theory of elementary particle physics, Oxford University Press, 1982, ISBN 0- 19-851961-3.
[46] Higgs boson: The 'god particle' explained|Space, https://www.space.com/higgs-boson-god-particle-explained.
[47] R. Penrose, On the gravitization of quantum mechanics 2: Conformal cyclic cosmology, Foundations of Physics, 2014, Springer.
[48] P. H. Frampton and S. L. Glashow, Chiral color: an alternative to the standard model, Physics Letters B, 1987, Elsevier.
[49] S. Hawking and R. Penrose, The nature of space and time, 2010, books.google.com.
[50] T. S. Grigera, V. Martín-Mayor, G. Parisi, and P. Verrocchio, Phonon interpretation of the 'boson peak'in supercooled liquids, Nature, 2003, nature.com.
[51] G. Parisi, Recent progresses in gauge theories, AIP Conference Proceedings, 1980, aip.scitation.org.
[52] K. T. McDonald, The Helmholtz Decomposition and the Coulomb Gauge, Joseph Henry Laboratories,

Princeton University, 2020, kirkmcd.princeton.edu.
[53] A. Chubykalo, A. Espinoza, R. A. Flores, A. G. Rodriguez, Helmholtz theorem and the v-gauge in the problem of superluminal and instantaneous signals in classical electrodynamics, Foundations of Physics, 2006 – Springer.
[54] S. Hossenfelder, S. Hofmann, M. Bleicher, and H. Stöcker, Quasistable black holes at the Large Hadron Collider, Physical Review D, 2002, APS.
[55] S. Hossenfelder, Physics beyond the Standard Model, https://citeseerx.ist.psu.edu.
[56] R. Iyer and E. Markoulakis, Theory of a superluminous vacuum quanta as the fabric of Space, Physics & Astronomy International Journal, 2021, 5(2):43–53.
[57] R. Iyer, Physics Formalism Helmholtz Matrix to Coulomb Gage, Oral PRESENTATION at the 6th International Conference on Combinatorics, Cryptography, Computer Science, and Computation, 2021, November 17-18th, and published proceedings pp.578-588. http://i4c.iust.ac.ir/UPL/Paper2021/accpapers/i4c2021- 1001.pdf.
[58] J. Bender and E. Zohar, Gauge redundancy-free formulation of compact QED with dynamical matter for quantum and classical computations, Physical Review D, 2020, APS.
[59] R. Iyer, Problem solving vacuum quanta fields, International Journal of Research and Reviews in Applied Sciences, 2021, 47(1):15–25.
[60] R. Iyer, C. O'Neill, M. Malaver, Helmholtz Hamiltonian mechanics electromagnetic physics gaging charge fields having novel quantum circuitry model, Oriental Journal of Physical Sciences, 2020, 5(1–2):30– 48.
[61] R. Iyer, C. O'Neill, M. Malaver, J. Hodge, W. Zhang, and E. Taylor, Modeling of Gage Discontinuity Dissipative Physics, Canadian Journal of Pure and Applied Sciences, 2022, 16(1), 5367-5377, www.cjpas.net. This paper introduces Hod Plenum* PDP assemblages role in ordered energy signals from noisy vacuum quanta.
[62] E. Markoulakis, A. Konstantaras, J. Chatzakis, R. Iyer, E. Antonidakis, Real time observation of a stationary magneton, Results in Physics. 2019, 15:102793.
[63] R. Iyer: Absolute Genesis Fire Fifth Dimension Mathematical Physics, Engineeringinc.com International Corporation, 2000, pp.63, Amazon.com.
[64] R. Iyer, and M. Malaver, Proof Formalism General Quantum Density Commutator Matrix Physics, Physical Sciences & Biophysics Journal, 2021, 5(2): 000185.
[65] M. Malaver, H. Kasmaei, and R. Iyer: Magnetars and Stellar Objects: Applications in Astrophysics, Eliva Press Global Ltd., Moldova, Europe, 2022, pp. 274, ISBN:978-99949-8-246-2.
[66] R. Iyer, Observables physics general formalism, Physics & Astronomy International Journal, 2022.
[67] R. Iyer, Configuring Observables Solving Physical Algorithm Quantum Matrix Gravity: Mini Review, Journal of Modern and Applied Physics, 2022, 5(2), 1-5.
[68] L. Randall, A. Shelest, and Z. Z. Xianyu, An Efficient Signal-to-noise Approximation for Eccentric Inspiraling Binaries, The Astrophysical Journal, 2022 - iopscience.iop.org.
[69] R. Iyer, Algebra Fields Time Transformations Geometry of Space Gaging, Oral INVITED SPEAKER PRESENTATION at the ICFAS2023 10th International Congress on Fundamental and Applied Sciences, 2023, June 8-10 in SPECIAL SESSION: ALGEBRA WITH APPLICATIONS.
[70] R. Iyer, Review force general conjectural modeling transforms formalism physics, Review Article, Physics & Astronomy International Journal, 2022, 6(3):119-124.
[71] L. Randall: Warped passages: Unravelling the universe's hidden dimensions, 2006, Penguin, UK.
[72] R. Iyer, M. Malaver, and E. Taylor, Theoretical to Experimental Design Observables General Conjectural Modeling Transforms Measurement Instrumented PHYSICS Compendium, Research Article, Research Journal of Modern Physics, 2023, 2(1):1-14.
[73] L. Randall and G. Servant, Gravitational waves from warped spacetime, Journal of High Energy Physics, 2007, iopscience.iop.org.
[74] E. Taylor and R. Iyer, Rethinking Special Relativity, Spacetime, and proposing a Discontinuum, PHYSICS ESSAYS 35, 1, 2022.
[75] M. Malaver and R. Iyer, Some new models of anisotropic relativistic stars in linear and quadratic regime, International Astronomy and Astrophysics Research Journal Volume 5, Issue 1, Page 1-19, 2023; Article no.IAARJ.98115, https://doi.org/10.48550/arXiv.2303.12161.
[76] M. Malaver and R. Iyer, Charged Dark Energy Stars in a Finch-Skea Spacetime, arXiv:2206.13943 [gr-qc], https://doi.org/10.48550/arXiv.2206.13943.
[77] M. Malaver, R. Iyer, A. Kar, S. Sadhukhan, S. Upadhyay, E. Gudekli, Buchdahl Spacetime with Compact Body Solution of Charged Fluid and Scalar Field Theory, https://arxiv.org/pdf/2204.00981, 2022,

ui.adsabs.harvard.edu.
[78] M. Malaver, H. D. Kasmaei, R. Iyer, S. Sadhukhan, A. Kar, A theoretical model of Dark Energy Stars in Einstein-GaussBonnet Gravity, Applied Physics, Volume 4, Issue 3, page 1-21, 2021 ISSN: 2664-0821DOI: https://doi.org/10.31058/j.ap.2021.43001, arXiv:2106.09520.
[79] M. Malaver, R. Iyer, Analytical model of compact star with a new version of modified chaplygin equation of state, Applied Physics, Volume 5, Issue 1, page 18-36, 2022, https://doi.org/10.31058/j.ap.2022.51002, arXiv preprint arXiv:2204.13108, 2022 - arxiv.org.
[80] L. Randall, Extra dimensions and warped geometries, Science, 2002, science.org.
[81] K. Jones-Smith, Identifying quasi-particles using non-Hermitian quantum mechanics using PT quantum mechanics, Philosophical Transactions - Mathematical, Physical and Engineering Sciences, 371(1989), 1-14, (2013).
[82] E. Taylor and R. Iyer, Discontinuum physics leads to a table of realities for making predictions, PHYSICS ESSAYS 35, 4, 395-397, 2022.
[83] R. Iyer, Quantum Physical Observables with Conjectural Modeling: Paradigm shifting Formalisms II: A Review, Oriental Journal of Physical Sciences, 2022, 7(2).
[84] R. Iyer, ALGORITHM OF TIME PRELIMINARY THEORETICAL RESULTS POINTING TO SPACE GEOMETRY PHYSICS TRANSFORMS, Canadian Journal of Pure and Applied Sciences, 2023, 17(2): 5673-5685, Publishing Online ISSN: 1920-3853, Print ISSN: 1715-9997, Online @ www.cjpas.net. This paper applies the Hod PDP mechanism to the analysis of time and space geometry and proposes a four-vector time matrix tensor algorithm to describe quantum gravity.
[85] R. Iyer, STRONG GRAVITY VERSUS WEAK GRAVITY: FIBER TRANSFORMS GRAVITY-BUNDLE - STRINGS: PRELIMINARY RESULTS, Canadian Journal of Pure and Applied Sciences, 2023, 17(2): 5697-5703, Publishing Online ISSN: 1920-3853, Print ISSN: 1715-9997, www.cjpas.net. This paper compares strong and the weak gravity via fiber transforms bundle strings, relating to Hod PDP mechanism and the micro-blackhole force.
[86] E. Taylor and R. Iyer, Einstein's questioning and speculations lead to theoretical photon momentum, PHYSICS ESSAYS 35, 4, 2022.
[87] E. Taylor and R. Iyer, How Einstein Prevents Bohr's Quantum Mechanics From Being A Fundamental Theory, PHYSICS ESSAYS 36, 3, 2023.
[88] E. Taylor and R. Iyer, How an electron can transit between energy levels without the atom emitting electromagnetic radiation, https://discontinuumphysics.com/sp/published-paper-7.
[89] S. Hossenfelder, Anti-gravitation, Physics Letters B, 2006, Elsevier.
[90] S. Hossenfelder et al., Signatures in the Planck regime, Physics Letters B, 2003, Elsevier.
[91] S. Hossenfelder, Phenomenological quantum gravity, AIP Conference Proceedings, 2007, aip.scitation.org.
[92] M. Malaver, R. Iyer, and I. Khan, Study of Compact Stars with Buchdahl Potential in 5-D Einstein-Gauss-Bonnet Gravity, Physical Science International Journal, Volume 26, Issue 9-10, Page 1-18, 2022; Article no. PSIJ.96077ISSN: 2348-0130, arXiv preprint arXiv:2301.08860, 2023, arxiv.org.

